DEPARTMENT OF ELECTRICAL AND ELECTRONIC ENGINEERING

Optical Characterisation of *Steatoda paykulliana* spider dragline silk

By

Sathiyapriya Ganesan

Supervisors

Dr. Kevin Webb

Electrical & Electronic Engineering

AND

Dr. Sara Goodacre

Life Sciences

March 2019

Project thesis submitted in part fulfilment of the requirements for the degree of Master of Science (by research) in Bio-photonics

The University of Nottingham

Abstract

This project aims to characterise the optical properties of spider silk under the non-destructive light microscopy technique. Spider silk is of interest to the bioengineering and industrial communities because of its mechanical and biomedical properties, such as being extremely strong , flexible and light conductive. Polarised light microscopy is a contrast enhancing technique used to quantify the optical properties of the birefringent materials. Using this method, the composition and three-dimensional structure of the anisotropic crystals can be investigated. Since spider silk is an anisotropic material, the optical properties of the silk and in particular the birefringence of the spider silk was measured using this technique. Initially, a simple optical microscope was constructed using Thorlabs components in order to evaluate the birefringence of the *Steatoda s*pider silk. Subsequently it was found that, the measurementof birefringence could not be calculated and the assembled system was not appropriate, as the silk indulged with different hydration conditions. Hence the optical properties of *Steatoda* spider silk under different environmental conditions were evaluated using the Olympus BX51 polarised light microscope. The research data acquired from the experiment were analysed using the statistical method. From the analysis, the proposed hypotheses were proved. such as significant difference in the value of birefringence within individual sample and between discrete silk samples. Also, substantial variance in thickness within individual silk sample and between distinct silk samples. Finally using data analysis, the value of birefringence under four different conditions were analysed and it indicated that the value of birefringence was varied to a great extent – it had a maximum value when the silk was in dry condition, the value decreased when the silk was in hydration; during dehydration the value increased again and in supercontraction, the value was drastically decreased. This is due to the fact that different environmental conditions affect the molecular assembly of the silk and this will possibly affect the properties of the silk.

Contents

LIST OF FIGURES

LIST OF GRAPHS

Chapter I

1.1 Introduction

Spiders synthesize protein silk fibres that have many beneficial properties such as it being lightweight, extensible, flexible and having exceptional tensile strength. The remarkable properties, Also, fascinate engineers to explore its potential applications in construction, medicine, textile, composites and even in the military [1, 2]. Spider silk has novel applications in bio medical research such as synthetic spider silk proteins can be used for coating implant devices made up of silicon and stainless steel [3] and for the production of bulletproof vests [4,5,6]. A research ‘A new route for silk ‘ by Omentto et. al shows that spider silk has new applications in photonic devices such as thin films , diffraction grating and organic photonic crystals [7, 8].

The silk also contains many expedient biomedical characteristics, such as having: biodegradability, antimicrobial [9, 10] and no allergic reactions to humans. These characteristics have attracted the medical field and has started to be tested, to make bandages [11] and sutures [12]. The biocompatibility [13, 14] and anti-inflammatory properties of spider silk [15] are ideal in tissue engineering, scaffolding, drug delivery and tissue regeneration [13, 16, 17]. Recent developments in the field of genetic engineering helped to reveal that there are possibilities to create artificial recombinant spider silk for biomedical applications. For example, to create artificial biomaterials, like: ligaments, cartilage, tendons, knee replacements and artificial nerves [18, 19, 20].

Many studies have been focusing on the mechanical properties of the spider silk. Spider silk has the ability to reflect UV radiation, this is particularly useful for the spiders to attract insects and other prey. [63]. A recent research on the optical properties of spider silk proves the capability of making this material for new applications in bio-photonics. The regenerated silk of *Bombyx mori* cocoons, casting a silk fibroin solution in an appropriate surface has been used to render

photonic devices, such as: light-emitting transistors, diffraction gratings and inverse opals photonic crystals [21, 22, 23]. Spider silk are far better than *Bombyx mori* cocoon silk regarding its strength and elasticity. Recently, light transmitting property of spider silk was proved by Huby *et al* in 2013. The research "Silk fibroin biopolymer films as efficient hosts for DFB laser operation" done by R. R. da Silva et al. figured out spider silk can also be used to design micro-optic fibres for optical bio-sensing [24]. The optical characteristics of the spider silk, is combined with other properties, such as: electrical [25], mechanical [26] and bio-resorbable, these can pave a way to new applications in various engineering fields [27,28,29]. Protein silk fibres have the capability of changing their material properties depending on their surroundings. This can be measured by collecting and analyzing particular parameters (phase, intensity or polarisation) of light when it is transmitted through the silk [30]. Tow, K.H., Chow, D.M., et al. explored the use of Native Spider Silk in 2018 and showed that it may be possible to make implantable devices, such as biosensors and bioresorbable waveguides. They have the ability to deliver optical power for optical therapy or imaging inside living tissues for medical analysis [31, 32]. These new applications that spider silk provides, are equivalent to the responsibilities that materials in mechanical devices offer; These future possible applications generates motivation to investigate further about the optical properties of the silk. Birefringence is one of the most important optical property [24]. Because, in general birefringent materials are used to control the light over different polarisation directions and is widely used to manufacture photonic components. As spider silk possess birefringent property, quantifying birefringence enables us to study the intrinsic property and molecular arrangement of the material. It could possibly replace the man-made engineering materials, in the field of medicine and optics.

Most of the research has been conducted on dragline silk of *Nephila clavipes*. However this research was focused on *Steatoda paykulliana* dragline silk as it has been studied much less than other silks. Spiders are spinning different kinds of silk so, studying other kinds of silks and their property will give knowledge about how the properties of the silks vary from one another and

how we can make use it for various potential purposes. As spider silk has significant applications in biological mediums, it is important to understand how optical properties will change with respect to different hydration conditions. Different treatment conditions are required in order to develop silk with a range of properties, suitable for different applications. The similar process is happening naturally in spider webs during raining. In general, spider webs, are usually attached to the support structures such as trees, garden furniture etc. When the silk is exposed to rainwater, it absorbs the water, this creates stress in the fibres. This stress is useful as, it aids the web to carry the weight of a raindrop.

The objective of this project was to determining birefringence of *Steatoda* silk in different hydration conditions and compared how far the experimental values are related to *Nephila* silk as previously determined by Ken N. Savage and John M. Gosline. Statistical Analysis was conducted to study the variations in each condition.

This section explains spider silk , brief description of spider silk glands, silk formation, spider silk protein and its structure. Also describes birefringence and significance of measuring the birefringence of the silk.

1.2 Spider silk

Spiders taxonomically belong to the Animalia kingdom and phylum Arthropoda, grouped within the class Arachnida and order Araneae [33,34]. *Steatoda paykulliana* comes under Theridiidae family and it is often referred to as the 'false widow spider' or the 'cupboard spider'. These names were given because, this spider builds its web in the dark or in isolated places such as sheds, under garden furniture and cupboards. These spices have reputation in UK for biting human. Spider silk is a protein-based, insoluble biopolymer and it has been recognised formore than two millennia [35,36]. The silk is produced by a specialised organ called, the 'spinneret'. The well-known Orb weavers, produces symmetric circular web with six different types of silk, each with distinct purposes and produced by distinct silk glands.

Steatoda produces sticky tangled web for capturing insects but never done any research before to study its characteristics of silk.

1.3 Spinnerets

Spinnerets are found on the base of the spider abdomen and are the main source of spidersilk [37]. Most spiders have six spinnerets, although the number of spinnerets varies among the different spiders, from two, four or eight. Silk glands attached to the spinnerets, produce different kinds of silk. Silk fibres can be thick or thin, dry or sticky, smooth or decorated with glue [38]. Spinnerets can move independently and each spinneret consists of many tiny spigots. The spigots have got a valve, the silks secreted from the gland comes out through the valve that controls the thickness and speed of the silk. Each gland, produces silk with different amino acid compositions, this differentiates the structure and properties of the silk. Figure 1.3 shows a scanning electron microscope (SEM) image,of the spinneret and spigots of orb-weavers, taken at the Nottingham Nanoscale and MicroscaleResearch Centre (NMRC).

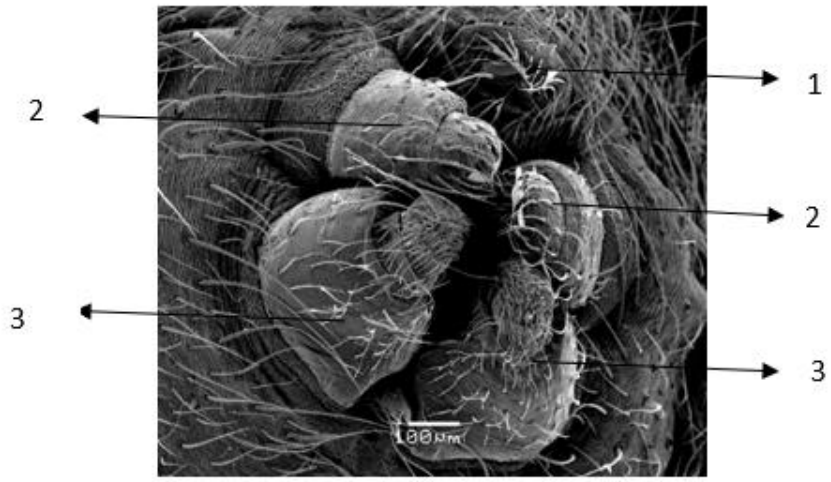

Figure 1.1: Spider Spinnerets. This figure shows the Scanning Electron Microscopic image of three pairs of spider spinnerets. 1. Colulus is a reduced cribellum (spinning orgaan) 2. anterior pair 3. posterior pair

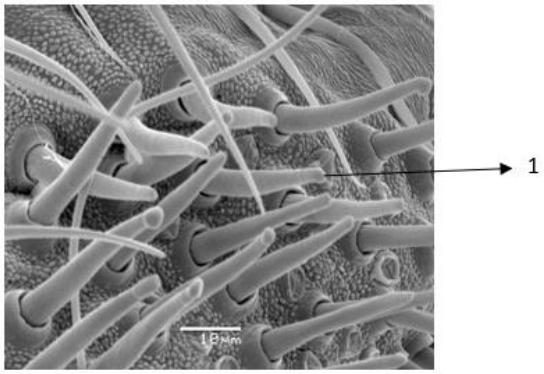

Figure 1.2: Spider Spigot. The figure shows the scanning electron microscopic image of spigots. Thousands of spigots are coming out from the spinnerets. 1. Microtubules – silk is coming out from this small tube

1.4 Spider silk glands

Spider silk is secreted by silk glands. The orb-weavers have seven distinctive silk glands, namely: major ampullate, minor ampullate, flagelliform, tubuliform, aciniform, aggregate and piriform [39,40]. Each silk gland produces distinct types of silk with distinct properties and functions. The ability to tune silk with different mechanical and material properties, depends upon the spinning process, storage conditions, silk composition, and extrusion process, drawing speed, prey [41], nutrition [42] and environmental conditions. The knowledge about spider silk glands, its spinning method and protein composition aids us to discover the properties of the silk. Orb-weavers have three paired appendages on their abdomen, which comprises hundreds of spigots, each attached to their glands. This arrangement equips a single spider with the ability to provide different kinds of silk. The major ampullate gland secrets dragline silk fibres, which are very strong and stiff. This is used for the framework of the web and for a lifeline. Dragline silk from the major ampullate, is indicated in Figure 1.1 as a red line on the web. The minor ampullate gland, which produces the radial lines and supports the spider's weight when it spins the web. The flagelliform gland produces the capture spiral, which is extensible, sticky and disperses the impact energy when an insect is caught on the web

[43]. The elastic properties of this silk helps to prevent such impacts from breaking or damaging the web. Aggregate glands produce glue dope, which is constituted by stickier and concentrated liquid drops [44]. Prior to spinning, silk dopes (silk in the form of thick liquid) are soluble and stored within the abdomen of the spider. These fibres are heterogeneous and semi-crystalline materials, which possess large and highly repetitive proteins. When extruded from the abdomen, the liquid silk dope experiences physical and chemical changes. For example: the pH level gradually decreases and forms insoluble fibres (43,44).

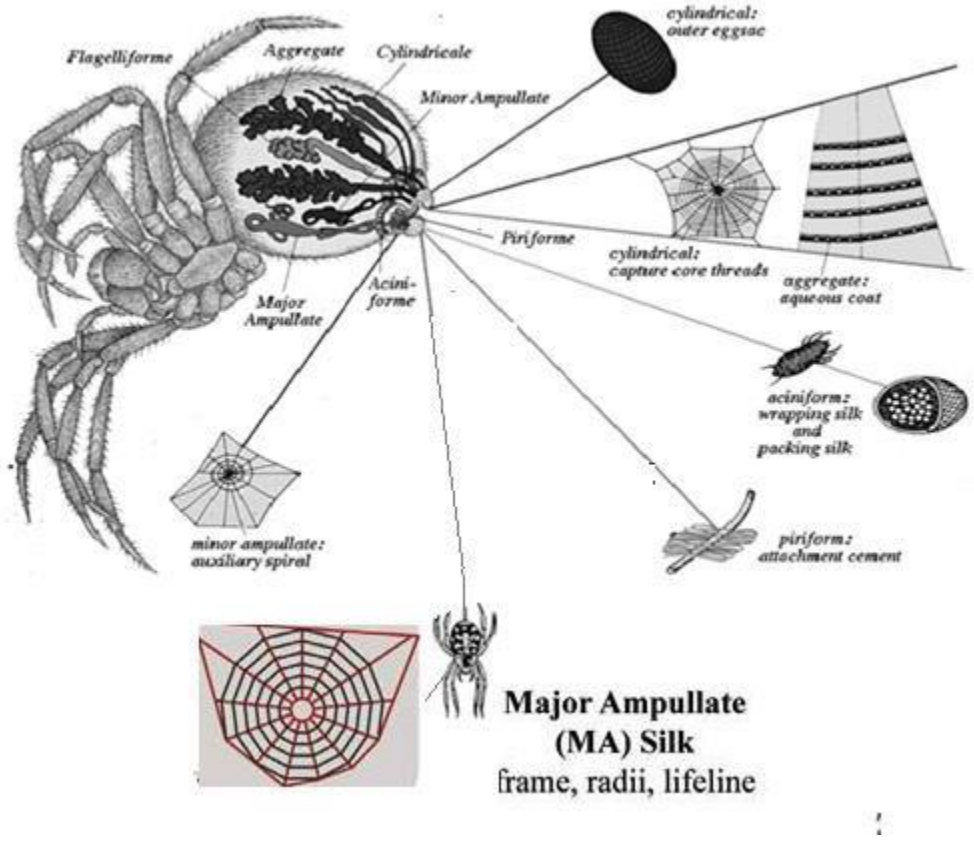

Figure 1.3: Illustrates seven types of glands and the silk they generate. 1. Major ampullate silk (dragline silk), minor ampullate silk, Flagelliform silk, aggregate silk, Cylindriform silk, Aciniform silk, pyriform silk. This figure was adoptedfrom the literature Kunal Singha et al., 2012 [42].

The above schematic diagram clearly indicates seven distinct kinds of glands and the silk generated form the spider. Major ampullate – Dragline silk, minor ampullate, - auxiliary spiral, aciniform – prey wrap silk and packing silk, periform – attaching cement, flagelliform – capture spiral, aggregate – glue dope and tubuliform or cylindrical gland – produces the tough outer

silk of the egg sacs.

The dragline silk is the toughest among the other six types of silks, as it is dragged behind the spider during its escape or when it falls from a height and thus usually denoted as dragline or lifeline silk. Orb-weaver dragline silk is five times stronger than steel and three times stronger than Kevlar [35, 45, 46, 47, and 48], and is able to stretch four times its original length [49]. Also, its torsional shape memory means, it can recover to its initial state without any external forces [37, 50]. The modulus (the ratio between stress and the strain of the substance) of *Nephila* silk, was about: 12.70GPa and the elastic strain (stress relative deformation) before breaking, was: 476%, when compared to the radii's mean extensibility of 39% [51]. The silk dissipates kinetic energy during stretching and relaxation. The amount of energy able to be absorbed per volume is higher than Kevlar due to its extensibility [52]. Orb-weaving spiders deposit glue patterns on their silk to catch their prey. This glue has strong adhesive strength, and it seems like a viscoelastic solid. It is highly sensitive and even reacts to humidity levels and the rain. [53]. For instance, the spider silk super contracts when it's very humid[37]. During super contraction, the silk on the web generates force which makes the unrestrained silk shrinks up to half its original length [37]. The absorbed water molecules, disrupts the hydrogen bond between the protein molecules and plasticizes the silk [38].

Silk glands have three sections, namely the: Secretory or Tail section, the Storage sac and the Spinning duct [54], as shown in Figure 1.2. The secretory section, secretes a highly concentrated protein spinning solution. This section has three zones, namely: A, B and C; in which, A and B are responsible for the spider silk protein secretion, called spidroin, and zone C is accountable for the regulation of the spider silk properties. The second section is the storage sac, in which the highly concentrated liquid dope is stored, and delivered to the spider silk when needed. This solution, moves through the funnel with ease, and attains a liquid crystal structure. This alignment of the crystal along the fibre axis, is responsible for the full-fibre formation [55]. The third section is a narrow duct, it contains a pump and valve system, and ends with a

spinneret. The *S*-shaped duct, eliminates water molecules from the protein content, subsequently it releases acids into the lumen; this lowers the pH level and solidifies the liquid substances [56]. Now the soluble liquid solution changes into insoluble silk fibres, and extrudes through a path called the spigot. The valve varies the diameter of the silk, which is present at the end of the duct [57].

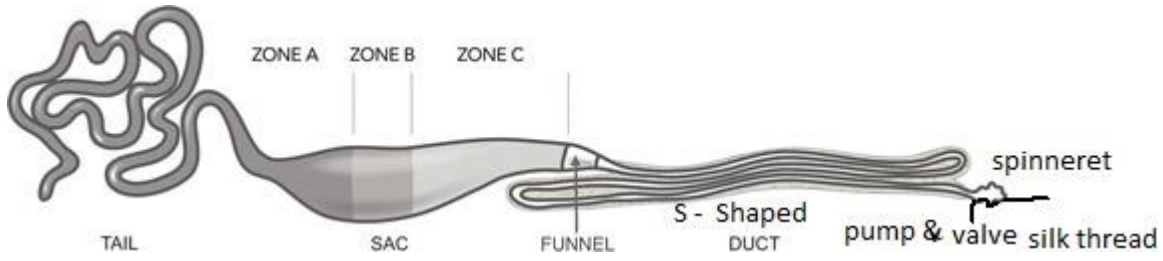

Figure 1.4: Structure of silk glands. This diagram was adapted from the Anderson. M. et al., 2013, [58]. 1. Zone A and B are responsible for spider silk secretion 2. Zone C fibroins are stored and stabilised 3. Duct – forming the silk fibres.

Figure [1.4] illustrates the silk-producing gland. It shows the different sections of the gland involved in extruding raw silk and polymerising the silk.

1.5 Spider Silk Composition

To understand the properties of spider silk , it is imperative to recognize the spider silk compositions, which are responsible for the silk. The spider silk consists of two components – the shell and core. The shell comprises of the glyco-layer, the lipid-layer and the skin. The core has an inner and outer area; The outermost lipid layer, is exclusively made up of lipids, with the absence of protein. The outer layer protects the silk from micro-organisms and the environment. [62]. The glyco layer is mainly made up of glycoprotein, and it is useful to extract water, when the fibre extrudes from the spigot [63, 64]. The skin proteins have a higher molecular weight, and are less glycosylated. The skin protects the silk from chemical agents, provides the silk with plasticity and acts as mechanical support, shielding the core fibre.

The core is composed of a special category of spider fibroins, called: ‘Major ampullate spidroin

I (MaSp1)' and 'Major ampullate spidroin II (MaSp2)',which is unique to the spider. Spider silk glands, have highly concentrated liquid proteins. During fibre formation, these are converted into solid proteins and are spread heterogeneously throughout the silk fibre [65].

Amino acids are monomers and they are basic building blocks of proteins. Every protein chain in spider silk, has approximately 20 amino acids. The order of amino acids, determines the properties of the protein. Spider silk protein has highly repetitive core domain sequences, and is bounded by non-repetitive terminals. They are built in a very specific way that makes the silk unique and attractive. The outercore is composed of β-sheets that lack spidroin II [66, 67]. B-sheets are a regularly ordered, secondary structure of protein. They are also composed of β-strands. β-strands contain amino acids with polypeptide chains. The outer core has a different protein composition to the inner core. The proline content obstructs the β-sheet and reduces the crystalline area [68, 69]. The inner core contains cavities, named: canaliculi [70, 71]; fibrils are formed in this region. In the outer core and fibril region, the molecules are oriented in a higher degree; this provides rigidness to the silk.

The space between the outer core and the fibrils, holds a high substance of MaSp2, and forms a less organised and more flexible medium [69]. Both MaSp1 and MaSp2 have an abundant amount of alanine and glycine residues, while proline is noticed only in MaSp2. MaSp1 has three categories of small peptide motifs, such as: the poly-alanine (poly (A/GA), glycine-rich (GGX, X is either leucine, tyrosine or glutamine) and non-repetitive amino/carboxyl termini. MaSp2 differs in the presence of proline residue that accounts for about 15% of the total amino acid content.The MaSp2 structural motif is composed of: poly A/ poly (GA) and GPGXX domains with a non-repetitive amino /carboxyl terminus (72). Alanine and glycine are known to promote β-sheets, while proline disrupts this formation and produces β-spirals in the amorphous region of the silk. Thus, MaSp1 is involved in the formation of the β-sheet crystalline region. Additionally, the β- spirals produced by MaSp2 in the amorphous region, connect with the β-sheets. ;Poly-A and GA are arranged in an antiparallel β-pleated sheet. The amide-to-amide

interaction among the protein back-bone, renders a crystalline region. This β-sheet region is embedded in the amorphous region,which is expressed as GGX in MaSp1, –GPGXX in MaSp2, 3_1- helical and type II β-turn. [73] These offer elasticity to the fibre. The poly-alanine sequences, provides hydrophobic nature, to the β-pleated sheets. Crystalline regions are made up of, less-ordered β-sheets and highly ordered β-sheets, in an antiparallel nature that provides stiffness to the fibre, while non-uniform amorphous regions give elasticity to the silk fibre [74]. Different kinds of silk, have different amino acid compositions and different properties.

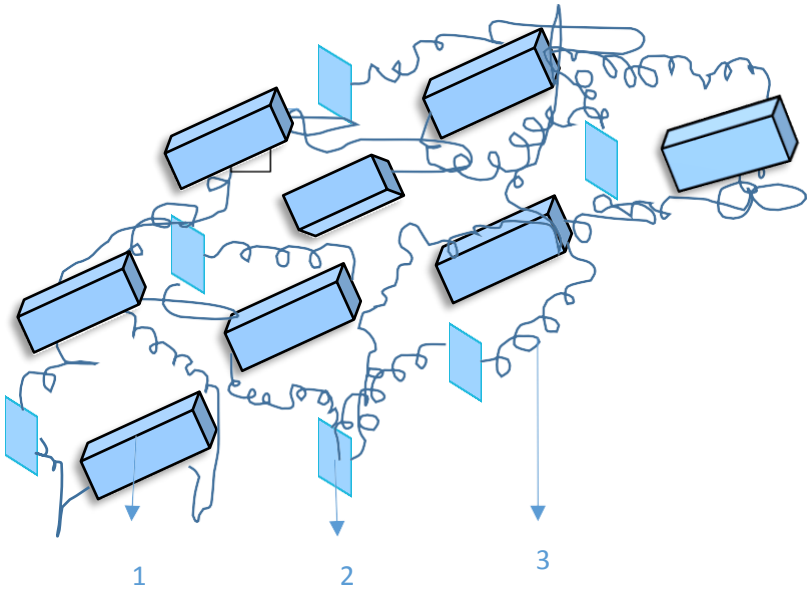

Figure 1.5: Spider silk structure Part 1 represents highly ordered β sheets, part 2 represents less ordered β sheets and part 3 represents an amorphous network chain.

Figure 4 shows the crystalline region, made up of highly ordered and less orderly stacked antiparallel β-sheets and amorphous regions. These crystallites are dispersed in the amorphous region. [75, 76]. β-sheets crystals are arranged in certain way inside the silk in three dimensions. Each material has its own index of refraction. Index of refraction is the way how the light propagates through the material. So understanding how the spider silk crystals refract the light will able to understand the way how the crystals are arranged inside the silk. Next section will explain how to calculate the index of refraction and birefringence of the silk.

1.6 Birefringence

Electromagnetic waves, consist of electric and magnetic, field vibrations that are perpendicular to each other. Also, the wave oscillations are perpendicular to the direction of the propagation. Electromagnetic light waves that have vibrations in more than one plane, are called unpolarised light waves, vibrations in a single plane are polarised light waves. The method of transforming unpolarised light into polarised light is called polarisation. There are several methods to produce polarised light.

1. Polarisation by reflection - When light is incident on a transparent surface, such as glass or water, the part of the light gets reflected. light gets polarised. If the light incident at a particular angle, called Brewster's angle, the reflected beam is completely plane polarised. Hence, the degree of polarisation, depends upon the angle of incidence.
2. Polarisation by scattering – When sunlight hits air molecules, its vibrates the electrons, perpendicular to the direction in which they are transmitted. The radiation produced by the electrons are polarised. Therefore, the light scattered by the air molecule, is polarised.
3. Polarisation by using a polariser - When unpolarised light is passing through a polarising filter, it emerges one half the intensity of the light and its vibrations are parallel to the axis of the polariser. They filtered all other vibrations. .The polarising microscope, uses the polarised light, to observe and evaluate the optical anisotropic properties of materials.

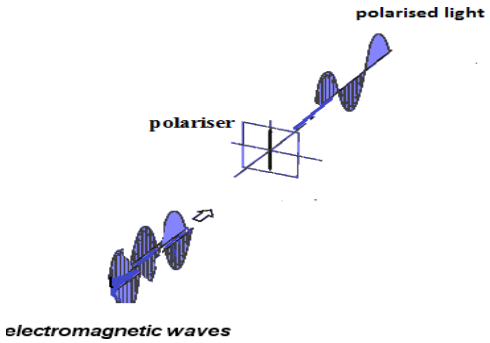

Figure 1.6 Electromagnetic wave

This diagram illustrates when an electromagnetic wave passes through the polariser whose vibrations are restricted in a single plane

4. Polarisation by refraction - When light passes from one medium to another, it either refracts or bends, this process is called refraction. Refraction changes the direction and the velocity of light, this is defined as: the ratio of the velocity of light in a vacuum (c) to the velocity of light in a medium (v). The refractive index depends upon the nature of the material and wavelength of light. It is represented as:

$$n = \frac{c}{v} \quad \text{Eqn (1)}$$

Isotropic materials such as glasses, possess refractive indices, which are uniform in all directions. Anisotropic materials, possess two different crystallographic orientations, which they refract light into two perpendicular components, with the direction of vibration mutually perpendicular to each other, this process called double refraction. Materials that possess this optical property, are called Birefringent materials and the phenomenon is called Birefringence. Spider silks are optically transparent and are naturally birefringent materials. These two orthogonally polarised lightstreams, travel with different velocities [78] and are oriented along the fast and slow axis. One iscalled an ordinary ray and another is called the extraordinary ray, which is represented in Figure (1.7). These two polarised light rays are experiencing different refractive indices – the refractive index n_e experiences an extraordinary ray and the refractive index n_o experiences an ordinary ray. The difference between these two refractive indices is called *birefringence (B)*,which is defined as: $B = ne - no$. Eqn (2)

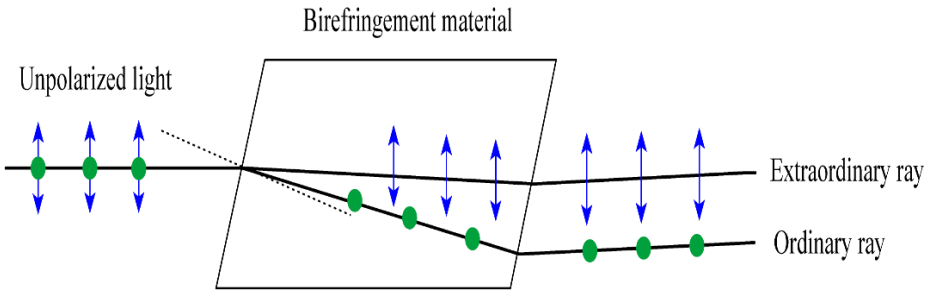

Figure 1.7: **Birefringence** - Shows the decomposition of unpolarised light into ordinary and extraordinary rays

1.7 Birefringence of spider silk

During the extrusion process, the optically isotropic spider silk liquid that is secreted inside the gland, is transformed into an anisotropic three-dimensional, liquid crystal. Spider dragline silk, is made up of β-sheet crystals and glycine-rich amorphous regions. The β-sheet crystals are aligned along the fibre axis and form a slow axis of birefringence, which is created by the relative alignment of constituent domains. The amorphous region, provides the ordinary refractive index (n_o); the crystalline region, provides the extraordinary refractive index (n_e). The different arrangements in the crystalline axes, produces differences in their refractive indices; this produces birefringence in the material. Hence, the birefringence of the silk material, depends upon, the difference in the refractive index value of the semi-amorphous region and the crystalline region. Birefringence can be used to provide a bulk measure, of the average orientation of the molecules [79]. Preferential orientation of the β-sheet crystals along the fibre axis, increases the birefringence of the silk material.

1.8 Principle of polarised light microscope

Polarised light microscopy, is a non-destructive microscopic technique, used to study the optical properties of birefringent materials. It equipped with the special components called 'polariser' and 'analyser'. In the microscope, the light from the light source passess through the condenser then it moves forward to the polariser. The polariser transmits light in a single direction while blocking the waves in other directions. The polariser only transmits light in vertical vibrations. The light passes through another polariser (analyser) which transmits light in vibration directions that are horizontal. As this is perpendicular to the initial polariser all light is blocked. The intensity of light coming out from the polariser is completely blocked by analyser. The variation in angular light intensity with analyser rotation, was explained by, Malus' law, which states: "The intensity of the light (I) coming out from the analyser is proportional to

$I = I_0 \times \cos^2\theta$ Eqn (3) [78]."

The output light intensity is bright and dark for every 180º rotation of the analyser. If both the polariser and analysers axis are at either 0º or 180º then the output is bright. If the axis are at either 90º or 360º then the output is dark. We can see brightness when the vibration axis of the polarizer, is parallel to the analyser.

When the birefringent sample is introduced between polariser and analyser, it splits the light into two orthogonal polarised electrical components, since the birefringent material has two refractive indices. When these two components passes through the analyser, they recombine and produce, constructive and destructive interferences. This makes the images of the birefringent material, more colorful and attractive. As spider silk samples are birefringent biopolymers, they can be characterised by polarising microscope, which can then be used to quantify the value of birefringence. This polarised light gets passed through the specimen and goes through the analyser which has a vibration transmission axis that is oriented 90º to the direction of the polariser.

1.9 Methods used to measure the optical properties of the silk

This section explores recent studies on the optical properties of spider silk. It analyses different methods, which are employed to measure the refractive index and the birefringence of the spider silk material. This also explains, how the other optical characteristics are evaluated. Furthermore, it provides the birefringence values for different spider silks.

Little and Kane deployed the index matching method, [80] to find the refractive index of radialsilks from *Plebs eburnus* spider silk. In this method, silk samples were positioned on a glass slide and the cargille refractive index oil, was slowly dropped onto the silk, until it was

submerged. Two or more calibrated liquids, were used where the samples refractive index lies, between the refractive index of those oils. Measurements were made at different polarisations directions. This was done by placing a polariser with the transmission axis, parallel np or perpendicular ns to the silk. To attain a precise value of the refractive index of the silk, different sections of the same fibre, were immersed into the refractive index oil. The refractive index, was matched when the contrast of the silk/liquid interface was minimised, this led to the silk appearing dark. A variety of Cargile refractive index oil, (A, AA) was used, this has calibrated refractive indices from, 1.40 to 1.64. MATLAB scripts were then employed to find the maximum contrast of the silk. The contrast of the silk was measured by, the difference between the intensity of background grey scale level and minimum grey scale level. The birefringence of the *Plebs eburnus* spider, was calculated using the formula: $\Delta n = np - ns$, this was calculated as ($\Delta n = 0.0129 \pm 0.0007$). However, the accuracy of birefringence measurement using this method, is limited. Little and Kane developed a new technique called the, 'hybrid immersion-polarisation method' [81]; this is a modified version of the image contrast immersion. This method is better because it is: faster and more accurate. Using trial and error, they tried different refractive index oils, most refractive index values were relatively the same, as the refractive indices of the silk fibre. To begin with, the silk was dipped in a refractive index oil, which its refractive indices was falling between the principal refractive indices of the spider silk. The polarised light was passed through the silk and then measurements were taken, when the orientation of light was parallel and perpendicular to the axis of the silk. The silk-oil index match, was measured. This was the consequence of orientation of polarisation. Similarly, the silk was immersed in different types of refractive index oils and the corresponding parallel and perpendicular orientations were measured. The silk was then washed with isopropanol, before being dipped into another refractive index oil; this is because it cleans the oil and does not affect the index of the spider silk. In this method, the value of birefringence also measured as a function of strain. The silk was mounted between the teeth of the Vernier Caliper. The strain

was applied by adjusting the distance between the teeth of the Vernier. The strain optic coefficients were also determined. 0.040 ± 0.009 and 0.026 ± 0.008.

Chow, Tow and their team (2018), demonstrated the optical behaviour of *Nephilia edulis* dragline silk [30]. The propagation loss, was measured by the estimation of the attenuation coefficient. They proved spider silk could propagate light in air and biological media. Furthermore, they integrated the silk fibre with a photonic chip and with an optical hybrid device; they combined both synthetic polymer and spider silk. The optical properties of spider silk, such as: spectral transmission, propagation loss and birefringence, were evaluated to explore its potential in the field of optics. Spectral transmission loss, was determined by sending lasers (infrared broadband radiation 800 – 880 nm) into the spider silk through a single-mode fibre. The output was measured using an optical spectrum analyser. The transmission loss spectrum, revealed that spider silk would transmit light up to 1400nm, with a transmission loss of 0.4 ± 0.2 dB/mm and 0.9 ± 0.2 dB/mm in the visible and O-band wavelength regions.

A wavelength-scanning method, was used to measure the birefringence of *Nephilia edulis* spider silk [30]. The spider silk was exposed to humidity, using a polarimetric setup. The SOP of the light was recorded. Variations in the level of humidity, changed the SOP (state of polarisation) of the light. Similarly, when the silk was inside the chamber, it was exposed to CO2, and the corresponding SOP of the light was measured. There was a variation in SOP due to the CO2 present in the chamber. This confirmed that silk can sense different chemical components, as well as humidity conditions. This study, proved that silk fibres, can be deployed as biochemical sensors and bio-compatible optical components. This paves the way for using silk as fibre-optic biosensors.

Holland and O'Neil (2012), explored the relationship between birefringence with stress, using the *Nephila edulis* dragline silk [82]. This investigated super-contraction-birefringence and Stress-Strain-Birefringence. They used a polarised light microscope, (MP 3500 BL) for the measurement of birefringence. Images were captured using a monochrome digital camera and

transferred to a PC, for analysis. Metripol software was used for the analysis, it produced computerised images and it gives both quantitative and qualitative information. The software measures the retardation δ of the silk.

Retardation is defined as

Equation (4) $\delta = L(n_1 - n_0)\mathrm{K}$

Where $\mathrm{K} = 2\pi/\lambda$

λ - wavelength of the light, L is the diameter of the silk fibre in micrometers.

Birefringence is defined as calculating *L* and *K,* and substituting the value into equation 3; this gives the value of birefringence *B*. This study is closely related to the thesis, as it measures the birefringence of silk in dry, wet and supercontraction conditions, using a polarising microscope.

Savage and Gosline (2008), studied how proline affects the mechanical and optical properties of *Araneus* and *Nephila* dragline silk, under dry and hydrated conditions [83]. In their experiment, the specimens were examined using a polarising microscope, with a rotating stage at 45° between two crossed polarisers. A Wild de Senarmont 546nm compensator, was used for calculating retardance measurements. The analyser rotated until extinction was attained. The Birefringence was then measured from the retardance value. The mechanical and optical properties of the silk weremeasured in dry and hydrated conditions. In the hydrated state, the birefringence of the *Nephila* silk was decreased by 50%, the *Araneus* silk was decreased by 75%. Dry *Nephila* silk, displayed approximately 50% more birefringent than the *Araneus* silk. This study, was one of the first to speculate about the molecular alignment of both, the *Nephila* and the *Araneus* silks, based upon their optical properties, as measured by birefringence.

1.10 Aim of the project

This project aims to measures, the birefringenceof the silk in dry conditions and it also measures the extent to which the silk was contemplated,to alter its optical properties depending upon the different hydration conditions. This research, analyses and interprets the experimental value of

birefringence, of the silk under different treatments using statistical analysis. Moreover, this study shows how the silk alters its optical properties, when it is exposed to different hydration treatments.

The following objectives were made, in order to study the optical characteristics of the spider silk:

1. To determine the birefringence of *Steatoda paykulliana* spider silk using a polarised microscope and to analyse birefringence under different hydration conditions.
2. To study the optical property of the silk, the optical system will be constructed using polariser and analyser, for controlling the polarisation state of light within the fibre. 4F optical system will be introduced to increase the contrast of the image and the images of the silk samples will be captured for different orientations of the polarisers.
3. The pilot study with *Nephila clavipes* dragline silk will be conducted since the silk was well characterised, where the relevant values of the birefringence of dry and hydrationof the silk were already published [83]. This known value will be compared with our experimental value. Sample size will be calculated using standard deviation, power and effect size in order to know the required number of samples for the experiment.
4. The birefringence of the *Steatoda* dragline silkwill be measured and it will be compared with the value of the *Nephila* silk.
5. The *Steatoda* silk will be exposed into four different conditions; dry, hydrated when restrained,dehydrated and super contracted and the measurements of birefringence will be made to analyse, how this alters and control the optical properties of the silk.
6. Statistical analysis will be conducted in order to analyse the variations of birefringence within an individual silk sample and between discrete silk samples.

1.11 Hypothesis

1. It is hypothesised that there will be variations in thickness and birefringence measurements within each individual silk sample as well as between discrete silk

samples.

2. It is hypothesised that there will be variations in thickness between two distinct silk samples namely *Nephila* and *Steatoda.*
3. When the silk is exposed to different hydration conditions: Dry, Hydrated, Dehydrated and supercontracted, it is hypothesised that the attribution of different hydration treatment of spider silk will alter the birefringence of the silk.
4. It is hypothesised that in a dry state the silk will have a maximum range of birefringence as the alignment of the molecules in a dry state is higher than the hydration state.
5. It is hypothesised that there will be variations in the birefringence of the silk depending upon the level of hydrations. If the silk absorbs water, it will alter the molecular alignment of the molecule also thus changes the value of birefringence.

Chapter II

2. The Birefringence Measurement of Spider silk

2.1 Introduction

Microscopes are optical devices, employed by researchers and medical professionals to view magnified images of small objects, with the help of visible light and lenses. Microscopes are classified into different categories based on image formation, light sources (some microscopes use visible light while others use laser beams, electron beams or sound waves etc.) and the nature of the sample used. We use different microscopes for different purposes. This study employs the usage of a polarised light microscope. The polarised microscope is ideal as, it provides a non-invasive, label-free bulk measurements of three-dimensional structures and the composition of an anisotropic specimen, by observing colour changes or image contrast using the polariser and the analyser with the consequence of birefringence.

This study aims to construct an optical system, to quantify the birefringence of spider silk under different environmental conditions. This chapter illustrates the design and how the Thorlabs

optical components are used for the construction of the system. Moreover, it explains how the images of *Nephila* silk samples, were taken using crossed polarisers. Furthermore, this chapter describes how the birefringence of the *Steatoda* dragline silk was measured.

2.2 Sample Preparation

Spider silk samples, were prepared from two spider species, namely: *Nephila clavipes* and a *Steatoda paykulliana.* These spiders were kept in the spider laboratory, in the School of Life Science at Nottingham University and are regularly fed crickets and water. Spiders were allowed to roam freely on corrugated black cardboard; from which dragline silk, was left naturally by the spider from their spigot. The silk was subsequently collected and placed across paper slide window card and attached by cyanoacrylate glue. The silk from two spiders *Nephila* and *Steatoda* were collected in order to compare the characteristics of known *Nephila* silk with unknown *Steatoda* silk. The size of the paper slide card, has the same dimension of microscope glass slide (75mm X 25mm). To avoid any contact with the microscope and glass slide, the silk was attached within the cut window.

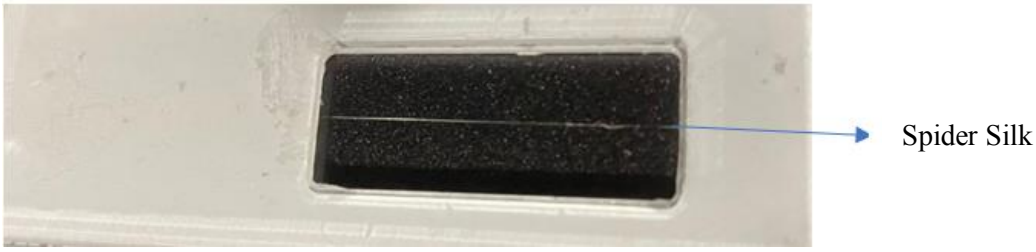

2.1 Paper slide card with cut window. Within the window the spider silk was attached. The dimension of the slide card id same as the paper slide card.

2.3 Construction of optical microscope

A plan was set out to design the microscope system. During this process various factors were considered. Initially, it was examined the variables that need to be measured with respect to spider silk birefringence. Different methods were analysed from the previous study to measure the birefringence quantitatively. Also, the suitable method to construct the optical system were studied. The limited timescale to complete this project were considered. After the method was

chosen, the layout of the optical system was drawn using the ray diagram. This layout, enhances the efficiency of the optical system, as it provides an indication of the prerequisite components and their locations, along with their functions. Then the complete set of source requirements such as optical, mechanical and biological (Silk samples) were analysed. Availability of the resources were checked and the resources were then requested to administer the study. The necessary components and their specifications were noted, then the designing process were broken into two stages – Stage 1 and Stage 2.

Thorlabs is a manufacturer who provides, a wide range of optical components and accessories that are optimised for the assembly of custom photonic and imaging applications. In stage 1 - the CMOS camera, tube lens, and the objective lens were planned to construct. Human hair was used as a test sample to optimise the microscope. In stage 2 – a condenser illumination system with 4F optics were planned to assemble the system and the spider silk samples were used for imaging. Finally, polarisers were attached to the optical system, to provide polarised images for the measurement of birefringence.

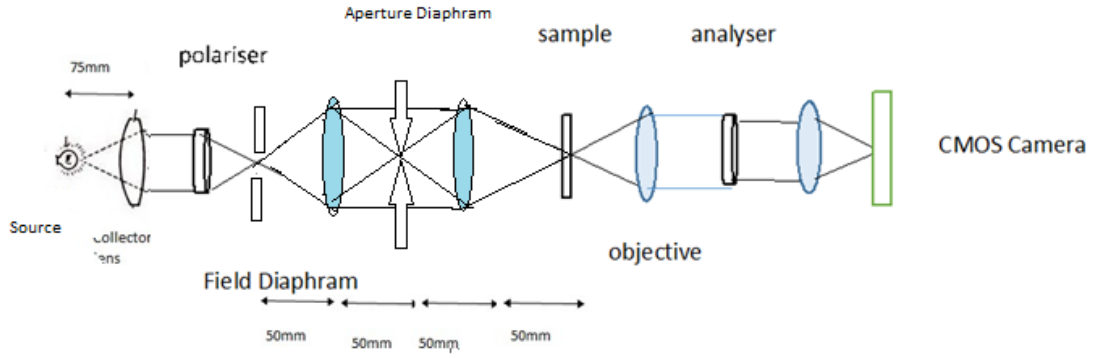

Figure 2.2: Design of optical system with 4f imaging

2.3.1 Required components and their specifications

This section, provides a brief description of the components that were used for the construction of the optical system provided. An optical breadboard with tapped holes, which was used as the platform to construct this optical system. In this configuration, a green LINOS bright High LED light source, with a centre bandwidth of 530nm, was used as the light source the current

stabilisation was 30mA, with a supply voltage of 2.8v [84]. Here, an Olympus plan achromat objective lens which has a numerical aperture of 0.4, with 20x magnification [85]. The dry objective worked well with the space between the eyepiece lens and the specimen. This plan objective lens, produces flat images and they get infinity-corrected, hence the rays coming out of the objective lens will be parallel. To observe the sample with fine details the sufficient contrast and the correct magnification are necessary. When considering magnification there is a limit for minimum and maximum magnification required for the details in an image that needs to be resolved. Beyond that limit we cannot able to resolve the image. Numerical aperture of the objective lens determine this limit. The total magnification of the microscope is a combination of objective lens and eyepiece lens. So, choosing objective / eyepiece combination is very important to get an optimal magnification of the sample without getting unnecessary artifacts. For this construction, the combination of 20X objective lens with 10X tube lens were used to produce 200X enlarged image of the spider silk.

In microscopy, the term resolution is defined as the ability of the microscope to distinguish minimum distance of the two distinct point of a specimen can be seen as two separate entities. Abbe was the first person who describe the resolution limit often referred as diffraction limit of the optical system.

According to Abbe the resolution limit of the microscope

Lateral resolution (LA) = $\lambda/2NA$(Eqn 5)

The resolution of the microscope depends upon the numerical aperture of the objective (NA) and wavelength of the light that was used to examine the specimen. Numerical aperture determines the ability of the objective to gather light. NA is an important factor to determine resolution and depth of focus. In order to increase the resolution, the sample must be viewed through the light with shorter wavelength and the objective with higher value of numerical aperture. Larger NA objectives collect wider range of light and producing higher resolution images. Here, the resolution of the optical system = $\lambda/2NA$

Substituting the value of wavelength and numerical aperture will provide the approximate value of lateral resolution required for the silk sample to resolve as LR depends upon other factors such as coherence of illumination, specimen type etc.

$LR = 530 \times 10^{-9} / 2 \times 0.4$

~ 0.66 um

So, specimen diameter smaller than this value (LR = 0.66 um) cannot be resolvable.

According to previous study, spider silks have varying in thickness along its length. The values are in few micrometers. The research done by Romer. Lin and Thomas Scheibel, 2008, the diameter of the spider silk was varied from 1um to 5um. The lateral resolution required for the spider silk should be at least 1um. But here the value was 0.66um. so the system has the ability to resolve the spider silk.

The camera used in this optical system was the DCC1645C (Thorlabs - New Jersey) which contains a colour CMOS sensor, with a frame resolution of 1280 × 1024 pixels and an electronic rolling shutter, controlled and powered through USB 2.0 cables [86]. Field diaphragm which positioned next to the collector lens was used to control the diameter of the light beam entering into the system and is imaged into the same plane as specimen. Aperture diaphragm was used to control resolution and contrast of the image. It has a slider to open and close diaphragm. Varying the size of the opening , change the cone of light projected into the specimen. Too much opening will allow more light into the specimen and make the image glare and results loss of contrast. Similarly, closing the diaphragm too much will allow small amount of light , increased diffraction and of loss of resolution. In order to obtain the right balance of contrast and resolution the aperture opening should be at an optimum level. The polarisers used in this optical system had a diameter of 25mm. This circular polariser was designed for a wavelength of 532nm. The polarisers have linear polarising films and anti-reflection (AR) coatings, which are on both sides of the polarisers. The cage plate was used to mount the optical components, Post holders were used to mount the optical components onto the breadboard via a tapped hole

in the cage plate. Iris diaphragms, Biconvex lenses, Plano-convex lens and C-Mount threads were used to assemble this system.

2.3.2 Construction of the optical system – Stage 1

An image acquisition software (ThorCam™, Thorlabs, New Jersey, USA) was installed into the PC, then the CMOS camera DCC1645C, was attached to the PC via a USB 2.0 cable; The camera was fixed to the cage plate using a C-mount thread. The four cage rods were inserted through the cage plate. After that, a biconvex lens was attached to another cage plate which was used as a tube lens. It was then slid into a position through the cage rods. Initially, this was aligned to focus an object from "infinity" (parallel rays) and capture the image on CMOS camera. In order to achieve this, the lens was focused out of a window at a distant object (trees), then the tube lens was moved back and forth to get an image of trees on the camera,. This method was chosen because, such a distance approximates infinity to the close focal distance of the objective chosen. If the object was at infinity, the image would be focused at the focal point of the convex lens, here the camera was placed at the focal point of the tube lens. Once it was positioned, the tube lens was fixed in place on the cage plate using small screws on the plate. Both cage plates were mounted on the post holder at the same height, thus fixing the optical axis of the system. Using a RMS thread lens mount, the objective lens with 20X magnification was secured and positioned on another cage plate. The sample was placed at the focal point of the objective, to obtain infinity conjugate imaging.

This led to the light coming from the objective, being parallel to the optic axis. Hence, the tube lens has parallel rays and focused the image at its focal point. Initially, human hair was used as a testsample. It was fixed on a separate movable cage plate and positioned in front of the objective lens. The sample was illuminated by the LED light source, which was placed on a separate post holder. The distance between the sample and the objective lens was adjusted

until, the image of the sample was visible on the camera.

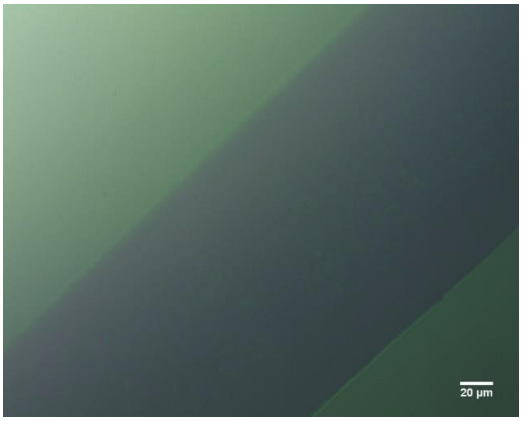

Figure 2.3 Image of human hair with critical illumination

.A 200X magnified image at the plane of focus, was produced with a 20X objective and 10X tube lens. Using the software ThorCam , the obtained images were saved on the computer system as a TIFF file. All the components needs to be positioned in the same height.

2.3.3 Construction of optical system - Stage II

In the second stage of construction, 4f imaging system was designed to obtain efficient illumination and improve the resolution of the image. Here, a convex lens was placed in front of the LED light which functioned as a collector lens and two convex lenses with the same focal length were used to construct a 4F imaging system. Figure 2.3 illustrates the layout of the 4f imaging configuration.

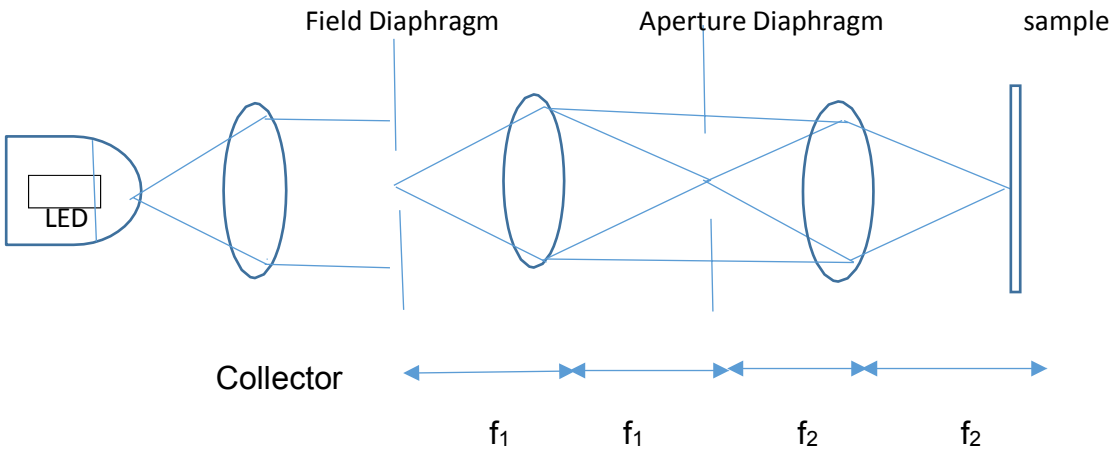

Figure 2.4 Schematic diagram of 4f imaging system. The source was placed at the focal point of collector, field diaphragm was placed at the focal point of biconvex lens aperture diaphragm was positioned between the focal point of pair of convex lenses.

To place a source at the focal point of the collector lens, the image of the source was initially captured on a small piece of paper. After getting a sharp image, the distance between the source and the collector is measured which was 75mm, that is the focal length of the collector. The collector is now attached to the cage plate and positioned at the same distance of the focal length 75mm from the LED source. It captures the utmost possible emitted light and collimates it into the light path. Four cage segment rods were attached to the collector cage plate . On the other side of collector lens , the field diaphragm was positioned and slid through the cage rod. Using the lens mount, a pair of biconvex lenses with a focal length of 50mm, was attached to the cage system. The first 50mm lens was positioned 50mm from the field iris diaphragm (i.e. at the focal point of the lens). In order to regulate the diameter of the illumination, the image of the field diaphragm was made fallen onto the sample. After that, a second matching lens with the same focal length of 50mm, was added to the cage system and the distance between the two lenses were adjusted to 100mm (i.e. two focal lengths away from the first – forming a "4F" system). The area in between the lens is called Fourier plane. The Fourier transformation of an image is like a diffraction pattern, where low frequency components are located close to the optical axis and higher frequency ones are placed farther away from the origin. Placing filters will only allow low frequency components close to the optical axis and removing high frequency components.

Here an aperture diaphragm was placed 50mm away from both lenses, this is at the meeting point of the focal lengths of two convex lenses (i.e. Fourier plane). This Aperture diaphragm, limits the diameter of light passing through the Fourier space, thus acting like a variable low-pass spatial filter that adjusts the numerical aperture of the illumination. This 4F configuration, provides an image of the field diaphragm, to the sample with a 1:1 magnification, because the focal lengths were matched. Images of the hair samples were captured by the camera using this improved illumination (4F) arrangement. Figure 2.4 shows the image of the hair. Due to the

ambient light falling on the camera the background appeared bright and reduced the contrast of the image. It was rectified in the next step of the construction process. by covering the system with a black sheet enclosure.

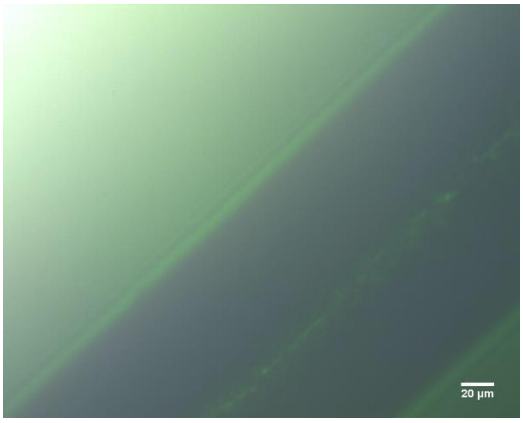

Figure 2.5 Image of human hair with 4f assembly.

2.4 Spider silk under polarised light

Next, two polarisers were introduced in the light path. The first polariser was positioned in the fourier plane after the collector lens. The second polariser (analyser) was positioned before the tube lens. Both the polariser and analyser can be rotatable. Analyser was rotated until the field of view appeared dark. In this position both polarisers were aligned perpendicular to each other, (i.e.) vibrational axis set 90° apart, the light intensity that encounters the analyser was blocked. The sample of *Nephila* spider silk, was introduced in the light path that was fixed on the stage using sticky tape. The transmission axis of the polariser is perpendicular to the silk length. The image of the silk was observed and captured by the camera. When the analyser got rotated clockwise, the rotation of polarised light by the birefringent sample, produces variable contrast to the specimen. This is because when the polarised light passes through the silk, it splits the light into two orthogonal components - an ordinary ray and an extraordinary ray. The retardance produced by the extraordinary ray, passes through the analyser and produces an image of the silk.

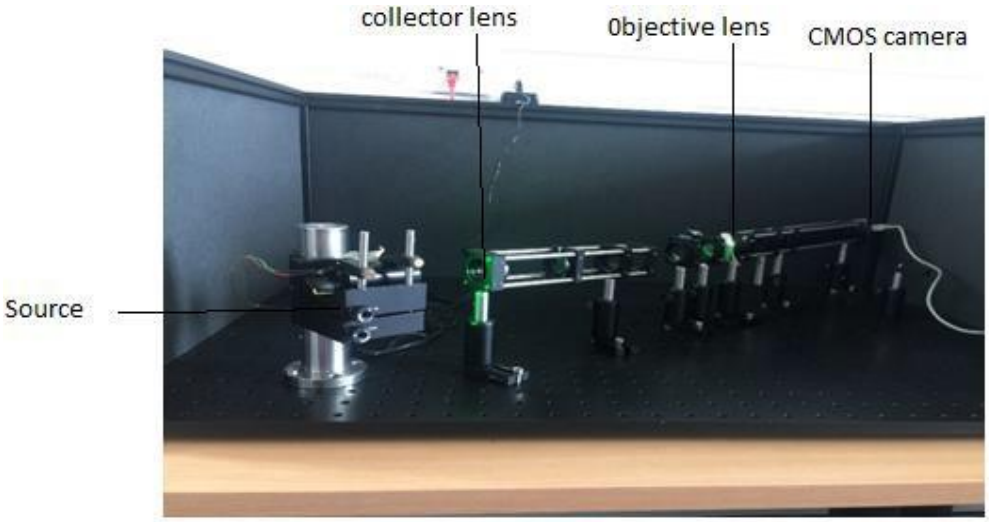

Figure 2.6Assembled optical system. The picture shows optical bread board, green LINOS LED light source, collector lens, objective lens and camera.

Both polarisers are able to rotate 360º. For every 45º rotation of the analyser, the image of the silk either brightened or diminished.

The intensity of the light coming out from the analyser, is equal to: $I_a \sim \sin^2(2\Theta)$ - Eqn (6)

$I_a \sim \sin^2(2x45°)$

$I_a \sim \sin^2(90°) = I$

The output intensity is high when the silk is at an optimum angle of 45º with respect to polariser and analyser.

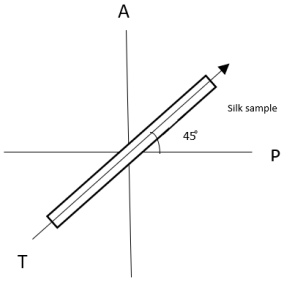

Fig : 2.7 The sample's position between polarisers. It was positioned in which the axis of transmission (T) at 45° between crossed polarizer (p) and analyser (a). The image appeared bright against dark background.

Fig 2.7 shows when the silk sample was placed with its transmission axis 45° between crossed

polarizer (*p*) and analyzer (*A*), light vectors in the slow axis is retarded more than the light vectors in the fast axis which are right angles to each other. These two vectors recombine, some of which is transmitted to the analyser and make the image appear bright against a dark background.

Extinction occurs when the vibration axes of the silk aligned with either polariser or analyser axes. These extinction positions, define the directions of vibration axes of the silk. Because when the plan of polarisation lined up with one of the axes of the silk, the light simply goes through the silk as plan polarised light, because the other axis perpendicular to the direction and then the energy coming out from the analyser has no energy. Output energy depends upon, the sample birefringence and the angle of the analyser. These two factors, influence how the light gets transmitted through the analyser.

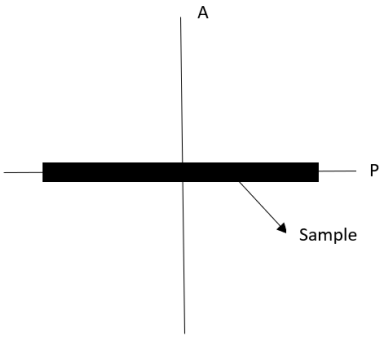

Fig: 2.8 Sample positioned parallel to the polariser. When the sample positioned with its transmission axis parallel to the polariser between crossed polariser (a) and analyser (A) it appears dark .

Fig 2.8 shows silk's extinction position when it's transmission axis is placed parallel to axis of polariser. When the silk axis is either parallel oº or perpendicular 90ºto the one of the axes of the polariser or analyser then the output intensity is zero. For other angles the light energy will be minimum, however, at 45º the output intensity will be maximum.

The image of the *Nephila* silk, were taken under polarised light. In Figure (2.9), the image of the silk was bright. This indicates that the silk was aligned at a particular angle between the polariser.

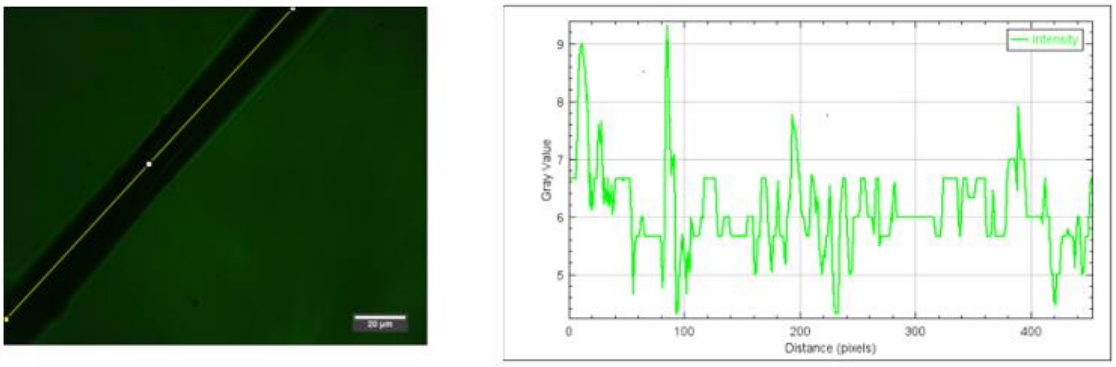

Figure 2.9 Image of spider silk under polarised light with a line profile graph. In this figure, the green dark image represents the image of the *Nephila* silk. It was at an particular angle to both polarisers.

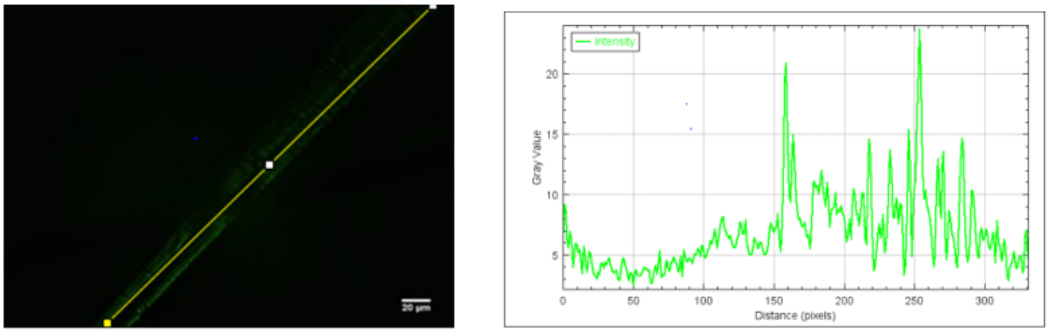

Figure 2.10: Image of the silk in which the polarisation vibrations are perpendicular to the analyser . The line profile graph shows the intensity of light that passes through the analyser. The intensity is very low until 150 pixels after that the intensity increased gradually. It has two peaks one at 160 and another one at 250 pixels.

Images 2.9 and 2.10 were taken using the same sample, light illumination, numerical aperture and magnification. But , in those images there were variations in the intensity of light . Line profile graph represents the light intensity distribution of the image. In the graph, the grey value represents mean value of all pixels with in selected area. When comparing both graph the intensity is relatively low in image (fig 2.10) and is not uniform. Some places are bright other places are dark. The height of the peak represent how many pixels of certain intensities are present in that image. The first image (fig 2.9) is bright and the intensity distribution is relatively higher than the second image (fig 2.10).

2.5 Measuring the birefringence of the silk using BX51 Olympus Polarising LightMicroscope

The constructed optical system lacked the sensitivity of measuring refractive properties of the silk samples and failed to capture quantitative data to demonstrate anything unambiguously. So, there was a need to reconduct this observation with an enhanced commercial system. The commercial apparatus are superior in performance, due to its more intricate and refined design. This section, describes the implementation of the experimental set-upin detail. Furthermore, it explains how the birefringence of the *Nephila* and the *Steatoda* dragline silks were measured under normal and hydrated conditions.

2.5.1 Polarised microscope configuration

The Olympus BX51 transmitted light microscope, was utilized for the subsequent measurements, as illustrated in Figure 2.8.

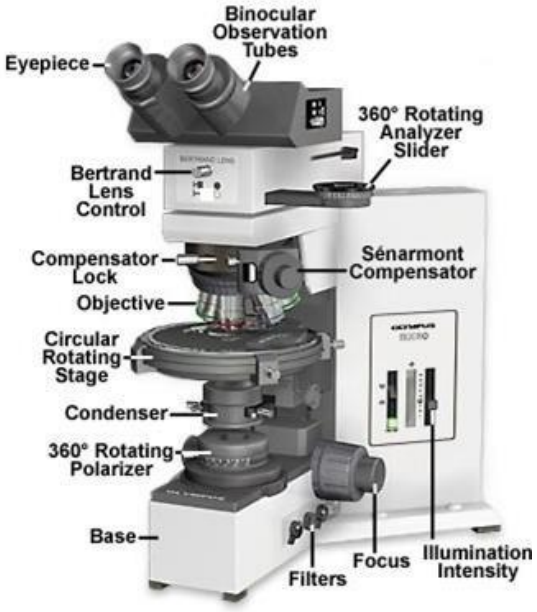

Figure 2.11: BX51 Polarising light microscope. This figure was adapted from the website[87]. Labels are clearly demonstrating the parts of the microscope- Where the polarised is positioned, circular rotating stage, condenser, compensator lock, eyepiece.

The stabilised tungsten-halogen light source had a power of 50W was attached to the base of the microscope. This provides light to the sample via the collector lens, field iris and condenser which was combined with an aperture diaphragm. The intensity of the light, can be adjusted by

brightness adjusting knob. The voltage was indicated on the side of the lamp. The microscope has a rotatable circular stage with a specimen holder along with graduated scales from 0 to 360°. The objective and condenser in the microscope are strain-free. Strain free objectives specially designed for polarising microscopes to reduce aberrations over the entire field of view. The rotatable nosepiece, provides the user with the desired objective magnification: 10X (0.25NA), 20X (0.40NA), and 40X (0.65NA). The eyepieces in the microscope (10X) are adjustable depending upon the users inter-pupillary distance. An efficient polariser, is secured beneath the condensers assembly and a rotatable analyser U-AN360P (Olympus Corporation Japan) is fitted in the middle of the intermediate tube, after the objective lens but before the tube lens. It has vernier scale markings, which indicate the angle of orientation of the analyser in the light path. In use, the transmission direction of the analyser, is oriented 90° to the polariser. This is to extinguish the light transmitted by the polariser. The retardance produced by the sample will be measured by the compensator. Compensator positioned in the intermediate path, of a microscope.

2.5.2 Berek compensator

The Berek compensator, is used to quantitatively measure the optical retardance of the materials. It increases the sensitivity of the polarising microscope, to detect material with low birefringence. It specifies where the birefringence is present in the material. It measures retardance from 0 to 11,000nm value. Fig 2:9 shows the Berek compensator.

Figure 2.12 Berek compensator. It clearly shows microscope optical axis orientation, compensator crystal, Graduated scale, Tilt angle indicator, Compensator plate tilt adjustment dial This figure was adapted from the website [88]

The Berek compensator is equipped with highly birefringence calcite crystal which operates by measuring the rotation angle of that optical plate cut perpendicular to the optical microscopic axis. The figure 2.10 shows a calcite plate positioned in a rectangular frame.

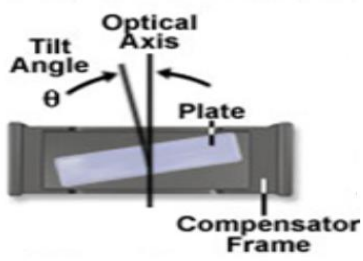

Fig 2:13 Compensator frame with Calcite crystal. It shows tilt angle with respect to optical axis. This figure adapted from the website [88]

It is attached to a rotating drum with the vernier scale, which indicates the tilt value. Initially the scale reads 30º when the plate is positioned horizontally. At this point a large dark cross appear in the field of view. The centre represents the optic axis of the calcite, the cross represents vibration directions of polariser and analyser. If the drum is rotated the light coming out from the compensator, interfere each other and produces primary, secondary and subsequent black stripes appear one after another, for white light interference colours appear. When the plane polarised light from the polariser propagate through the birefringent specimen it changes the polarised light into elliptical polarised light. Because the specimen has two refractive index axis so light split into two electrical components. They have different amplitude and they differ in phase by 90º. These elliptical waves from the specimen falls onto the birefringent compensator crystal and the plate is rotated perpendicular to the light beam to produce polarised light of variable ellipticity. When these elliptical components from the compensator is opposite in direction of rotation and equal in dimensions to the elliptical components produced by the birefringent object, then the light coming out from the compensator is linearly polarized in the plane of the polarizer. This will not be transmitted by the crossed analyzer. Here the retardance produced by the specimen is compensated by the calcite crystal inside the compensator. If the birefringent plate is perpendicular to the microscope optical axis; now the compensator plate acts as an ordinary

isotropic material and exit no polarised light.

However, when the compensator adjustment dial is rotated, the polarised light passing through the crystal alters its velocity. The retardance of the polarised light is dependent upon the angle of tilt and wavelength of light. The light perpendicular to the incident plane travels through the compensator's ordinary axis without any velocity change. Light from the extraordinary axis, gets retarded furthermore and gives out an additional phase shift. This is because , when the slow axis of the compensator gets aligned with the slow axis of the sample, this increases retardance and consequently the birefringence. In contrast, when the slow axis of the sample oriented with the fast axis of the compensator, decreases birefringence. The additional phase shift produced by the compensator is defined by the thickness of the birefringent plate, wavelength of illumination, the refractive index difference between ordinary and extraordinary axes of the compensator and the tilt angle.

In practice, the silk was placed on the rotating stage and turned to an angle of 45º, with respect to the direction of the polariser and the analyser. The silk will appears bright with a dark background. Birefringence attains maximum value when the sample was positioned at 45º with respect to polariser and analyser. Then the compensator will be introduced and it is rotated clockwise direction until the middle of the sample attains extinction. The retardance produced by the specimen is compensated by the berek compensator when the axis of the specimen has aligned with the axis of the compensator. So, the retardance of the specimen equal to the retardance of the tilt angle, measured from the vernier adjustment of the compensator mechanism. Reading are taken from the indication on the scale. Now rotating the knob in the counter clockwise direction, makes the centre of the specimen dark, providing a second reading with the inverse sign. Taking the mean of these two readings gives the average tilt angle required, to compensate the birefringence of the sample. By using the reference table supplied by the manufacturer, the retardance value (δ) was calculated for the corresponding tilt angle. The birefringence of the specimen was determined by dividing this retardance value by the thickness of the specimen..

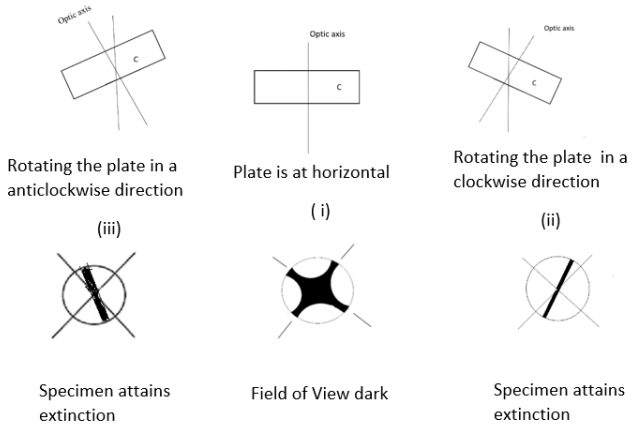

Fig 2.14 Position of compensator with respect to silk (i) when the compensator is at horizontal position, field of view and the optic axis (ii) extinction position of the specimen when the compensator is rotated at clockwise direction (iii) extinction position of the specimen when the compensator is rotated at counterclockwise direction

2.6 Measurement of birefringence of *Nephila clavipes* spider silk

To start with, the birefringence of *Nephila clavipes* spider dragline silk in a was determined as the value of birefringence of *Nephila* silk in a dry, hydrated state, had already been determined (83). This known value was compared with the experimental value of *Nephila* silk in a dry state Then the known value was compared with experimental value of *Steatoda* silk. The microscope was set up and the illumination system was turned on. The silk samples were then placed horizontally across the rotating specimen stage. Next, the silk was aligned to the centre of the cross hair reticule, then it was clamped in place by using a slide clip. The 10X objective with NA 0.25, and 10X eyepiece was selected because higher magnification decreases the contrast and made the image blurry. The specimen was focused by using fine and coarse focusing knob. A GXCam-5 (GT-vision, Stansfield) digital camera, was connected to the microscope using a c-mount adapter.

The light path of the microscope was specially optimised for establishing Köehler illumination. First, the light source was focused onto the sample. Next, the field diaphragm was closed until the edge only to be viewed. The image of the field diaphragm was focused onto a sharp edge,

using the condensers height adjustment knob. Condenser screws were adjusted to bring the circle of light into the middle of the view. The field iris diaphragm was then opened, until the circle of light filled the field of view.

The analyser was inserted into the light path then the microscope was carefully adjusted until the polariser transmission axis was perpendicular to the analyser. This was achieved by, rotating the polariser knob until the field of view becomes dark. The *Nephila* silk was positioned on a rotating stage then the stage was rotated 45° anticlockwise. In this stage, the intensity of light was increased with respect to the polariser or analyser. The polarised light fell at 45º to the axis of the silk fibre. The polarised light coming from the fibre, is composed of two components 0º and 90º relative to the fibre axis. Now, the Berek compensator was introduced to the slot. The calcite crystal, which present inside the compensator produces variable additional retardance through the rotation of the crystal.The compensator rotating knob was set to a position of 30° because, the axis of the calcite crystal will be at 45° to either the polarisers or analysers axis, so it is aligned to the fibre axis.

The compensator knob was rotated both clockwise and anticlockwise direction, until the centre of the silk turned dark. The reading on the compensator scale was recorded and the images were captured using a GX capture 14097 camera. Taking the average of these two readings gives the tilt angle required to compensate the birefringence of the sample. Using the reference table, retardance value (δ) for the corresponding tilt angles was calculated. Using the ImageJ software, the diameter of the sample was determined.

The formula for retardance is $\delta = (n_e - n_o)\, d$ Eqn (7)

Where d is the thickness of the specimen and $(n_e - n_o)$ is the birefringence.

The formula for Birefringence (B) is B = Retardance / thickness of the silk Eqn (7)

Substituting thickness and retardance value, the birefringence of *Nephila* dragline silk were

determined. Eight silk samples were taken for this experiment. For each silk, 3 measurements were made along the length of the silk A, B, C as from the previous research by Todd *et al*. the thickness of the spider silk, was not uniform, there were variabilities within every single strand of the silk. More measurements increase the precision of the measurements. So, in total 24 measurements were made. The average value of thickness and birefringence of the *Nephila* silk were determined.

This biological variation requires careful quantifications in order to achieve accurate result as these variations gives uncertainty. The sample size was determined in order to find out the variations among the measurements. The sample size influence the precision and level of confidence on birefringence measurements. The calculated sample size value was used to set up the experimental design, of birefringence measurement of *steatoda* spider silk in different hydration conditions. Statistical analysis was conducted in order to test the hypothesis. This section explains the effective validation of the hypothesis, which was formulated earlier of this study.

A one-way analysis of variance (ANOVA) was used to compare the mean of more than three categorical group mean and within each group there may be three or more levels of observation. It was conducted by using SPSS software applications, to examine the variation in thickness of the *Nephila* spider dragline silk in a dry state. It was found that there is a difference in thickness between 8 samples also within each individual silk and between discrete silk samples. (3 places were taken into account for this analysis).

Thickness

	Sum of Squares	df	Mean Square	F	Sig.
Between Groups	23.302	7	3.329	7.104	.001
Within Groups	7.498	16	.469		
Total	30.800	23			

Table 1: Thickness of dry *Nephila* dragline silk

From the above data analysis, the confidence interval was 95% and the alpha was 0.05. The null hypothesis has validation, if 95% of the confidence interval has zero value that means there

is no significant difference regarding the thickness of the silk, the silk is homogeneous. Here, the p-value was calculated as 0.001, which is < 0.05. This suggests that there is significant difference in the thickness of the silk samples. This reject the null hypothesis and clearly illustrated that the thickness of the silk samples were varied. Even a single strand of silk is not having uniform thickness. The statistical analysis of variability in the thickness of the silk thread, ascertains that the silk is non homogeneous, and it proved the hypothesis which was set at the beginning of the study.

Similarly, one-way analysis of variance, was conducted for the birefringence of eight silk samples of *Nephila.* Table 2 shows the birefringence measurements of dry *Nephila* dragline silk.

Birefringence

	Sum of Squares	df	Mean Square	F	Sig.
Between Groups	.002	7	.000	5.321	.003
Within Groups	.001	16	.000		
Total	.003	23			

Table: 2 Birefringence analysis of *Nephila* dragline silk

Here p-value = 0.003, which is less than 0.05. which reject the null hypothesis. It shows that the birefringence of the *Nephila* silk samples were statistically significant. This proved the hypothesis that the birefringence of the silk, varied between discrete silk samples and also within each individual silk sample.

2.7 Sample Size Calculation

The sample size is the prime factor for any scientific experiment to attain precise measurements. The expected variance was used, to estimate the number of samples required to resolve the expected differences in the birefringence. The main factors that aid to find a sample size are: effect size, power, level of significance and standard deviation of the population. If there is a large effect size, then the experiment require smaller sample size, in contrast, if the effect size is small, then

it require a large number of samples. The standard deviation implies the variations in the value of measurements. If the SD (standard deviation) is high, there will be large variation in the measurements, hence a greater sample size is required. On the other hand, If the SD is small, then a small sample size is enough for the experiment because, the variation will be low. In our experiment, the effect size was calculated based on research conducted by Savage and Gosline [83]. The effect size, is the difference between the mean value of birefringence in the dry silk, (the control group) and in the supercontraction state, (the treatment group.) This was found from Savage and Gosline's findings. The effect size is the difference in variation of the mean value in the control group and the test group.

Here the effectsize is calculated by = the value of the birefringence of *Nephila* silk in dry condition – the value of birefringence of *Nephila* silk in the supercontraction condition.

According to their findings, the value of birefringence of the *Nephila* in the supercontraction state, was almost decreased by half. Therefore, for calculation purposes we consider that the value of birefringence of the *Nephila* silk during supercontraction is half the value of birefringence of the silk in dry state . The birefringence value of *Nephila* in the dry state, was calculated as: 0.0385. So, the effect size was calculated as: 0.0192.

The sample size was calculated using the formula:

$$n = 2 (Z a + Z1 - \beta)2 \sigma2 / d2 \qquad \text{Eqn (8) [89]}$$

n – Number of samples, $Z\alpha$ represents the Z score with an area of α. If $\alpha = 0.025$, then $Z\alpha = 1.96$ (an error is a 5% with two-sided effect)

β – Is the Type II error, 1- β is the power

If the statistical power is 80 % then. $Z_{1-\beta} = 0.8416$

σ – Is the standard deviation

Here, $\sigma = 0.0119$.

Substitute all the values in the formula

$n = 2 (1.96 + 0.8416)^2 \times 0.0119^2 / 0.0192^2$

$n = 2 \times (2.8016)^2 \times 0.0001 / 0.0192^2$

$n = 0.001 / 0.0192^2$

$n = 5.96$

It was calculated that the number of samples required for this experiment was approximately 6. It appears that the sample size is very low. So, for the experiment of optical properties of the *Steatoda paykulliana* dragline silk under different hydration conditions- dry, hydration when restrained, dehydration and supercontraction 10 samples were used. In supercontraction state only 8 samples were used for the measurements as 2 samples were damaged during experiment while handling the silk.

2.8 Birefringence of *Steatoda* dragline silk under treatment conditions

To start with, the birefringence measurements were taken on *Steatoda* dry silk, following that, the silk was manipulated with different hydration conditions and their corresponding optical properties were estimated with 10X objective and 10X eyepiece magnification setup. For each sample, three measurements were taken along the silk length in three random locations. The following section explains how the different conditions were applied and how the measurements were taken successfully for each condition.

2.8.1 Birefringence of *Steatoda* dragline silk under dry conditions

Ten *Steatoda* dragline silk samples were prepared. Following the same above procedure, (the measurement of birefringence of *Nephila*) the retardance of *Steatoda* silk was determined using polarising microscope with berek compensator equipment. For each individual silk thread, three measurements were taken in random locations: A, B and C. In total, thirty measurements were made. The images were captured using the camera and the readings were recorded. Using

ImageJ, the thickness of the silk was calculated. The average thickness of the *Steatoda* silk and standard deviation was evaluated. Substituting these value in equation 5, the birefringence of the silk was calculated. UsingSPSS, the variation in thickness and birefringence of the silk samples were analysed.

The one-way analysis of variance, was conducted for the thickness of 10 *Steatoda* dragline silk samples, three measurements for each sample.

Table 2 shows the variance in thickness of dry *Steatoda* dragline silk.

Thickness

	Sum of Squares	df	Mean Square	F	Sig.
Between Groups	7.183	9	.798	3.241	.014
Within Groups	4.925	20	.246		
Total	12.108	29			

Table: 2 Thickness of dry *Steatoda* dragline silk

The p-value was 0.014, which was less than 0.05. So, it was concluded that there were substantial variation in the mean thickness of *Steatoda* silk samples.

An independent sample t-test was conducted, which was to test the variations in the thickness of the two different spider dragline silk samples - *Nephila* and *Steatoda* silk. To analyse and test the hypothesis, 8 measurements for the *Nephila* silk and 10 measurements for the *Steatoda* silk were taken into account.

Similarly, an independent sample t-test was conducted to test the birefringence of the *Nephila* and *Steatoda* dragline silks. From the analysis, the p-value was: > 0.05. This shows that there were no significant difference in birefringence of the two spider silks in dry conditions.

2.8.2 Birefringence of hydrated silk when restrained

In the second stage, *Steatoda* silk samples were soaked inside a Petri dish, filled with distilled water for fifteen minutes. Both ends of the silk were attached to an intact slide card, which

prevented the silk to shrink. In general, when spider silk hydrated , its length shrinks and its volume increases. [90]. After 15 minutes, the sample was placed on the rotating stage of the microscope for measurement. The optical retardance of the hydrated silks, were measured for 10 samples. The thickness of the hydrated silks, were measured and their images were taken for each measurement. From these value the birefringence was determined for the hydrated silk when their ends were attached.

2.8.3 Birefringence of dehydrated silk

In the third stage, hydrated silk samples were dried up at room temperature in the spider lab for 24 hours.The birefringence measurement of 10 samples were taken, the values were logged, and the images were captured using a GXCam-5 camera. The mean value of the thickness and birefringence of the dragline silk in a dehydrated state were calculated.

2.8.4 Birefringence of the supercontracted silk

In the fourth stage of the experiment, the birefringence of the supercontracted silk was estimated. The dehydrated silk samples, were again soaked with distilled water in the petri dish for fifteen minutes. To initiate supercontraction, one end of the silk was detached from the slide card. The silk started to absorb the water, this made the silk to shrink. It was easily noticeable that the length of the silk had been reduced and its volume increases. This process is called supercontraction. The length of the silk in the initial and the supercontracted state, was precisely measured using ruler. The initial suspended length of the silk sample was 15mm. After supercontraction, the length was decreased substantially also there were variations in the length of each strand of silk sample. The value varied from 7mm to 8mm. Now, the silk was placed on the rotating stage of the microscope. Using polarised light the retardation of the silk was estimated and the value of the thickness of the silk was calculated. Using these two values the birefringence of supercontracted silk thread was evaluated.

The birefringenceof the silk in four different conditions were analysed using SPSS.

One-way ANOVA was conducted to test the hypothesis, “the silk alter its polarising properties when it subject to four different hydration conditions”. 1. Dry state – the silk naturally collected from the spider 2. when the silk was immersed into the water while both of its ends were attached to the slide card, 3, Drying up the silk for 24 hours at room temperature 4. The silk was immersed into the water with one end of the silk was detached from the slide card,which makes the silk to supercontract. The same silk samples were used for all of these four experiments. From this analysis, the value of p is 4.87E-13, , which is < 0.05. This evidence, to reject the null hypothesis and indicating that there were variations in birefringence between silk samples.

Chapter III

3 Results and discussion

This study demonstrates the optical characteristics of the *Steatoda* spider dragline silk, based upon the birefringence of the silk. This section exhibits the outcome of the research and the findings. Using statistical analysis, the results that were acquired from imposing the silk with distinct hydration states, were analysed and interpreted. Moreover, this section explains the effective validation of the hypothesis, which was formulated in the earlier stage of this study.

3.1 Thickness and birefringence of *Nephila* spider dry dragline silk

Figure 3.1 shows the *Nephila* spider silk under polarised light when the polarisers were oriented perpendicular to each other. The mean value of thickness of *Nephila* dragline silk based on 8 samples were found to be 5.14 µm ±1.15. Standard deviation of mean value of thicknes was calculated. Standard deviation shows the variability of the measurements and determines the precision of the data points. The measurements were plotted in the graph and it represents the variations

Figure 3.1: *Nephila* Spider silk in a dry condition imaged under a crossed polariser

in thickness of the silks. They varied from 3µm to 6µm and theses variations are statistically significant.

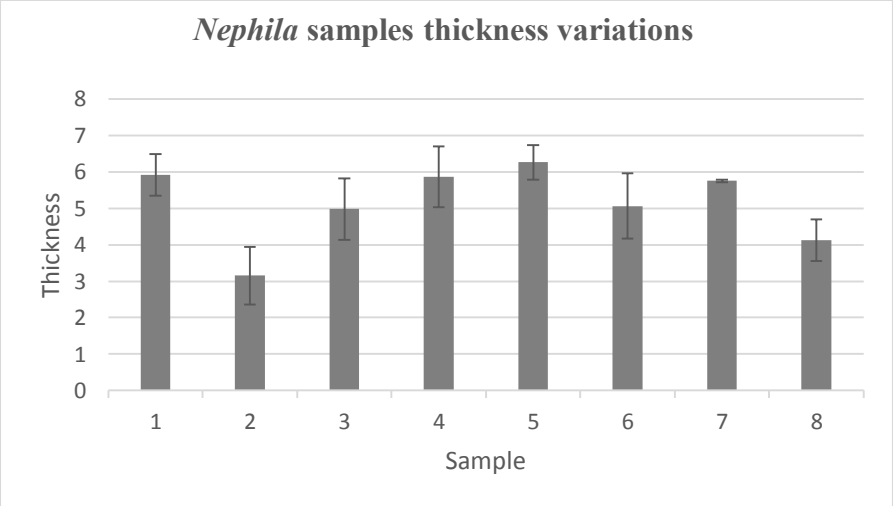

Figure 3.2 Graph showing the variation in thickness among the *Nephila clavipes* spider dragline silk samples.

The birefringence of the dragline silk from *Nephila* was (0.0265± 0.0119). Error bar represents variations of data points from the mean value..

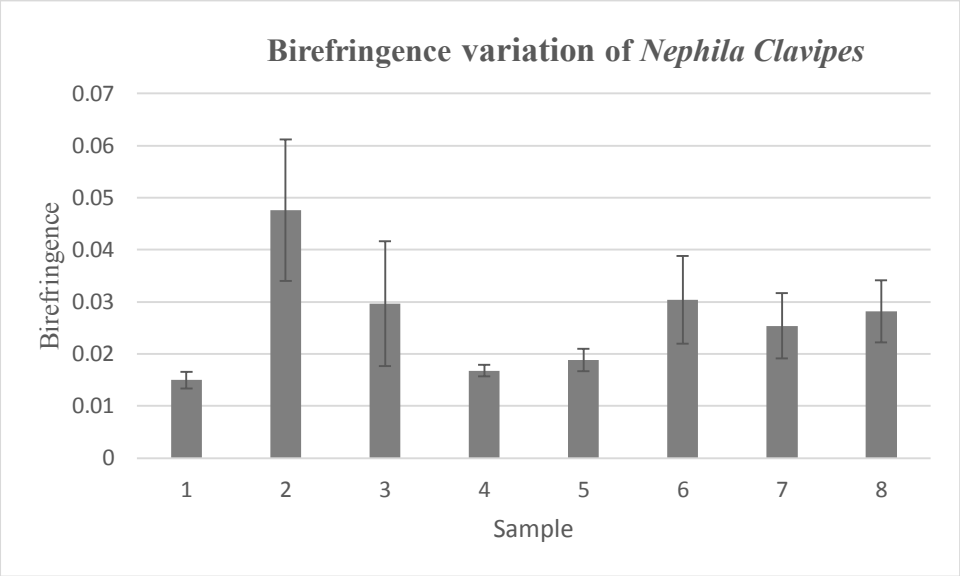

Figure 3.3: **Graph showing the difference in birefringence of *Nephila* dragline silk samples**

The value of birefringence found in this experiment was very close to the value that was obtained from Savage and Gosline in 2008, experiment as (0.0247±0.017).

3.2 Thickness and birefringence variations of *Steatoda* dragline silk under dry conditions

The mean value of thickness of the *Steatoda* spider dragline silk, was evaluated as 2.92±0.661µm. The mean value of birefringence of the *Steatoda* spider dragline silk was calculated to be: 0.0269±0.0095. From Standard deviation we understand that the variability of the data points are relatively small. Figure 3.4 shows dragline silk from *Steatoda* silk under extinction position. It occurs when the silk present within the first fringe and the retardance produced by the silk matching the retardance of the calcite crystal present inside the Berek compensator.

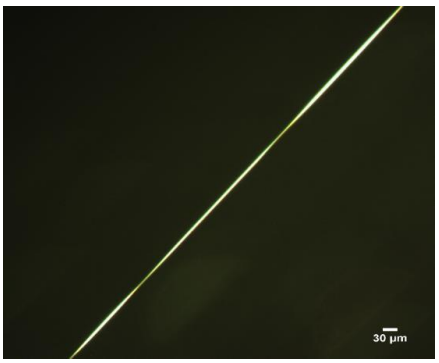

Figure 3.4: An Image of *Steatoda* dry dragline silk at extinction. The background was black as the polarisers were perpendicular to each other.

In the graph (Fig. 3.5) the error bar represents the natural variations in the thickness of each silk fibre, the variation implies that the spider altered the thickness of the silk, when it was extruded from the spigot.

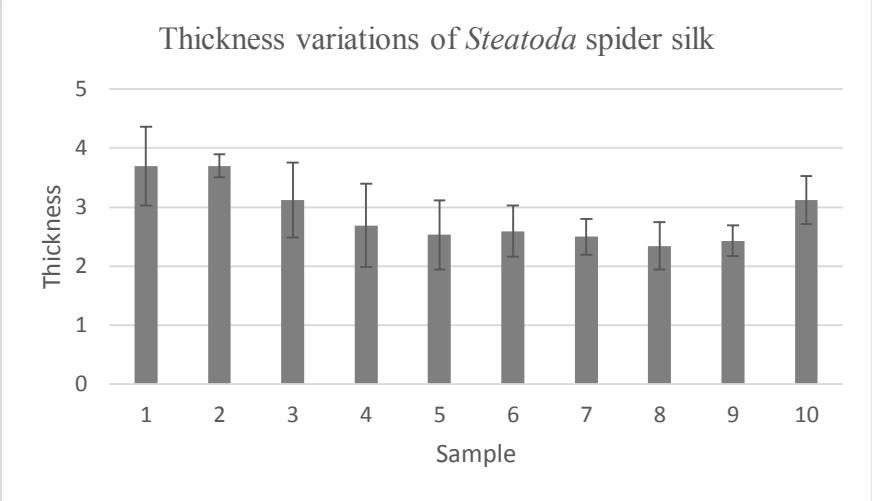

Figure 3.5: Graph showing the thickness variations of *Steatoda* dragline silk samples

Higher the thickness, higher the retardance. The higher orientations of β-sheets along the fibre axis, provides a greater refractive index and increases the value of birefringence [82]. The value of birefringence varies within individual silk and discrete silk samples.

The below graph shows the mean value of thickness of *Nephila* and *Steatoda* silk and indicating that the thickness of *Nephila* silk is higher than the *Steatoda* silk.

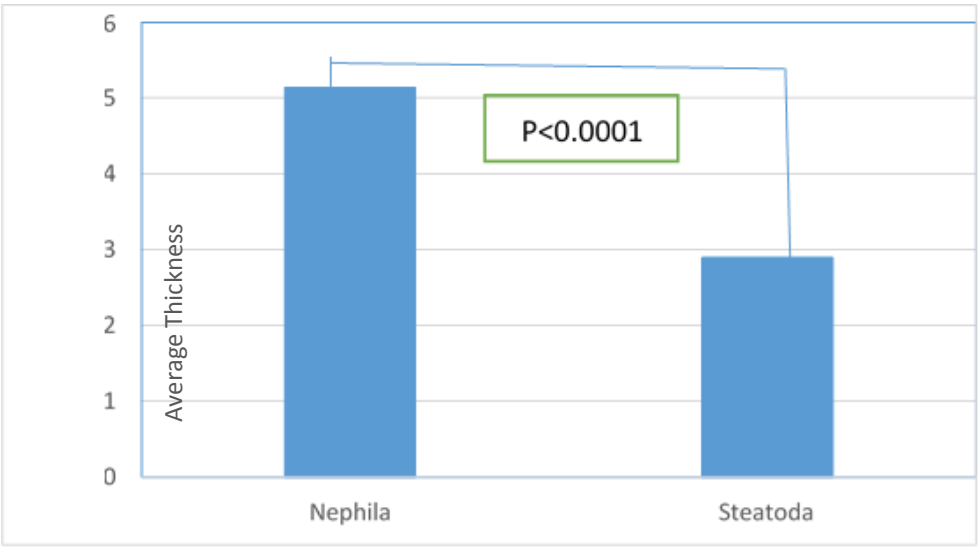

Figure 3.6: Graph showing thickness variations between *Nephila* and *Steatoda* silk under dry conditions

T-test has been conducted with respect to thickness variations between *Nephila* and *Steatoda*

silk and as p<0.0001. This shows significant variation between the thickness of the *Nephila* and *Steatoda* silk strands

The graph (Fig 3.7) shows mean birefringence of the *Nephila* and *Steatoda* silk.

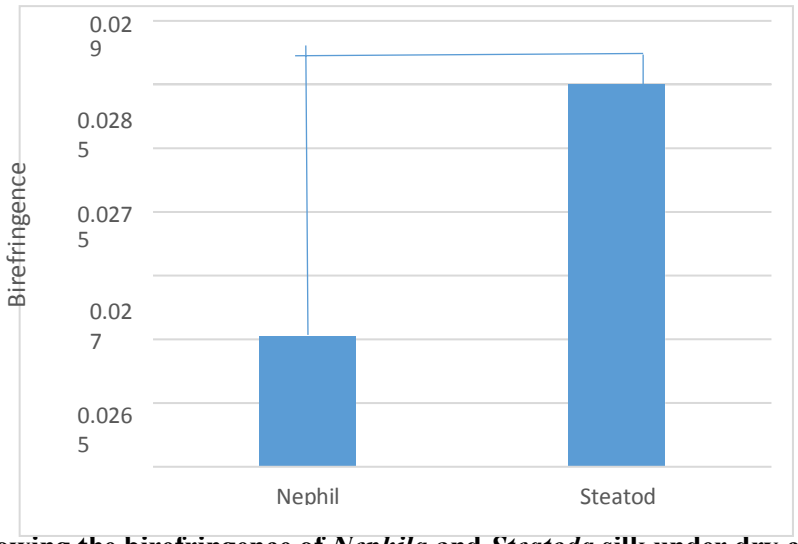

3.7 Graph showing the birefringence of *Nephila* and *Steatoda* silk under dry conditions

A T-test has been conducted for the mean value of birefringence of Nephila and Steatoda silks. P = 0.926 which is greater than 0.05, this shows there is not much difference in birefringence of *Nephila* and *Steatoda* silk. However, we can't conclude that the optical properties of *Steatoda* resemble *Nephila* in dry conditions. Because birefringence depends upon molecular arrangement. We have knowledge about the protein composition of *Nephila* dragline silk 81% -MaSp1 and 19% -MaSp2 [92]. But, *Steatoda* silk is not known yet. Need more research on molecular assembly of this protein fibre in order to be assertive.

3.3 Birefringence of *Steatoda* silk hydrated when restrained

From the experimental values, the mean thickness value of wet silk was calculated as: 3.21 µm± 0.485. Similar to *Nephila* , *Steatoda* silk also has variations in thickness. The mean value of birefringence of the silk was calculated to be: 0.0226±0.0048.

The value of birefringence of hydrated silk was dropped significantly. The below Figure (3.8) illustrates the hydrated dragline silk of *Steatoda,* when the silk got extinguished.

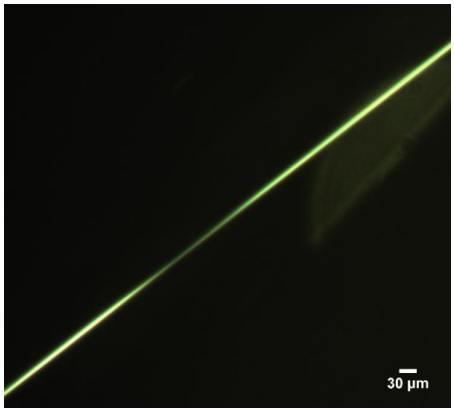

Figure 3.8: Hydrated silk under polarised light

According to the research findings, *Steatoda* spider silk chnges its optical properties depending upon the environmental conditions. From the previous study published by Savage and Gosline on 2008, the value of birefringence of *Nephila* silk in hydration state was 0.038±0.0014 (*N*=12). This indicates that *Nephila* silk has higher birefringence than *Steatoda* under hydration state. When the silk was submerged in water, the water molecules can penetrate into the silk and affect its molecular structure. So, may be *Steatoda* silk affected by water more than *Nephila* silk. Birefringence depends upon the complex molecular structure of the protein molecules along the fibre axis. This is strongly evidenced by Tillinghast and Chase (1984) and Rickel, Muller and Vollrath (1999) [93, 94, 95,]. This is particularly important because, the molecular structure characterises the properties of the silk. The absorbed water molecules, break the hydrogen bonds between the proteins and create a contraction bond [96], this then changes the amorphous region as they are hydrophilic in nature. If the percentage of absorbed water increases, it will affect the β-sheet network chain. Previous studies on the hydration of the silk, proved that spider silk loses its mechanical properties during hydration [97, 98]. "The effect of proline on the network structure of major ampullate silks as inferred from their mechanical and optical properties" by Ken and Savage, the birefringence of the hydrated silk was decreased by 10 – 15 % [83]. This proves that the naturally spun spider silk, responds to environmental conditions by changing its optical properties.

3.4 Birefringence of *Steatoda* silk when dehydrated

From this experiment, the mean value of thickness of the dehydrated silk was measured as 3.10μm±0.430 The mean value of birefringence of dehydrated dragline silk was calculated as 0.0255±0.0057.

The value of birefringence of the dehydrated silk was significantly greater than the hydrated silk but it had not reached the value of the silk in dry state. Figure 3.9 shows the extinction of dehydrated silk.

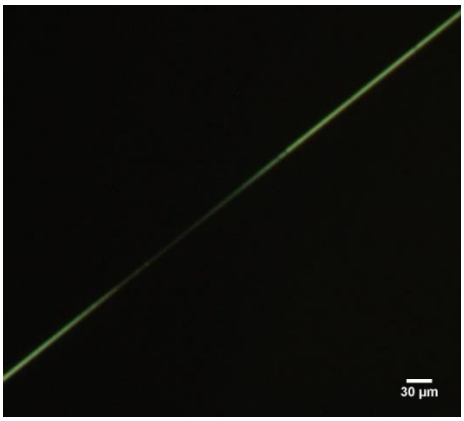

Figure 3.9 Dehydrated silk under a polarised microscope

During dehydration, water molecules evaporate, so the silk becomes dry and stiff. However not stiff like in dry state. May be the silk tried to come to its original dry position, which considerably increases the birefringence of the silk. During dehydration, the water molecules leaves the silk, so the contraction bond recedes and the hydrogen bond reformed. Consequently, the deformed molecules get re-aligned along the axis of the fibre, which increases the birefringence further. The silk tries to regain its original stiffness and optical properties however it still had a lower birefringence than a silk naturally in the dry state (0.0269±0.0095). This may be due to deformed protein molecules unable to return to their initial state.

3.5 *Steatoda* dragline silk under supercontracted state

In supercontraction state the mean thickness of the silk samples were found to be 5.10µm ± 0.410. The average birefringence of the silk in the supercontraction state was calculated as 0.0125±0.0009. The value of birefringence of *Steatoda* silk has decreased drastically, when compared to all other state.

Figure 3.10 shows the silk in a supercontraction state. The silk was in a relaxed state. The background was black as the silk was placed between crossed polariser.

Figure 3.10 Supercontracted silk under polarised light

During supercontraction as the silk shrunk and held more water , this causes to decrease the length of the silk and increases its volume. Water intake may alter the molecular arrangement of proteins significantly. The value of birefringence of the *Steatoda* silk in dry state was 51% more than in the supercontraction state. This finding, was similar to Savage and Ken's study regarding the birefringence of the supercontracted *Nephila* silk as, it halved accordingly. This evidenced that the *Steatoda* silk behaves similar to *Nephila* silk when it is in the supercontraction state. During this process, water was absorbed by a semi-amorphous region and affect the molecular structure of the spider silk, this resulted decreasing in birefringence. According to Chris Holland and Kathy et.al research on "Distinct structural and optical regimes in natural silk spinning," spider silk proteins, MaSp1 and MaSp2 vary with the amount of

proline they possess as, MaSp2 has rich in prolinewhereas MaSp1 has very low proline [83]. Proline in the polyalanine crystalline region is not affected by the water molecules; this makes the region naturally more hydrophobic. In contrast, the semi-amorphous region is rich in proline, which was affected by the water. Water molecules break the hydrogen bonds between the network chains and behave kinetically random coil, thus making this region hydrophilic [73]. Due to deformations in the semi-amorphous region, the silk shrinks and acts as an elastomer (elastic) [98]. Supercontraction, mainly occurs when the GPGXX motif re-organises[99]. Hence, supercontraction alters the orientation of molecules, which changes optical properties of the silk.

Due to humid atmosphere in the morning, the spider silk naturally gets hydrated and thus becomes supercontracted. During supercontraction stress builds up in the silk, which makes the web tight. Previous studies have shown that the restrained silk generates 40-50 MPa stress or above, depending on the humidity[17]. Another study demonstrated that the stress level depend heavily upon the rate of humidity. More stress is formed when the humidity of the environment increases rapidly. When the humidity decreases, the supercontraction stress also decreases.

If the environment gets warmer, the water molecules in the silk thread evaporate, making the silk loosen and change its molecular arrangement [100]. The research "Supercontraction of spider dragline silk for humidity sensing" by Zhihai Liu shows that supercontraction property of the silk, will be beneficial for sensor technology (101). The study "Exploring the use of Native Spider Silk as an Optical Fiber for Chemical Sensing" by Tow, K.H., Chow, D.M., et al., 2018. suggests that the silk is highly sensitive and will respond quickly to the surrounding environment, such as air molecules (CO2) and polar components like water. Another study shows that spider silk does not require any chemical processing, it can be used for sensing elements in its natural condition [26].

Table (3) summarises the experimental results of the birefringence of dragline silk under different hydration treatments.

Different states of the silk	Thickness(um)	Birefringence
Nephila dragline in normal dry state (n=8)	5.14±1.15	0.0265±0.0119
Steatoda dragline in normal dry state(n-=10)	2.92±0.661	0.0269±0.0095
Steatoda dragline silk in hydrated state (n=10)	3.21±0.485	0.0226±0.0048
Steatoda dragline in dehydrated state (n=10)	3.10±0.430	0.0255±0.0057
Steatoda dragline in supercontraction state (n=8)	5.01±0.410	0.0125±0.0009

3.6 Thickness and birefringence variations of *steatoda* dragline silk under different hydration conditions

Graph 3.11 shows the thickness variation of *Steatoda* silk under four different conditions.

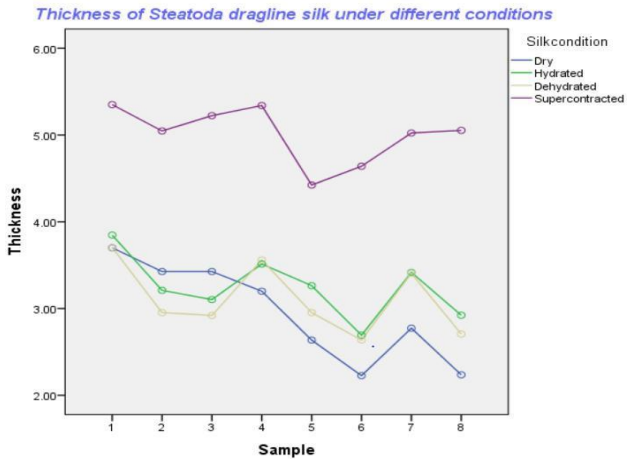

Figure 3.11 Thickness variations of *Steatoda* under four different hydrated states

From the graph, it was understood that in a dry state the thickness of the silk was low as the silk was stiff and retain more molecular order. In hydrated silk the thickness of the silk was increased as the silk absorbs water. In dehydrated state the thickness of the silk decreased ssignificantly. In supercontracted state the silk swell upon hydration and thickness of the silk was increased drastically.

Figure (3:12) represents the variations in birefringence and it clearly shows how the birefringence varies in each state.

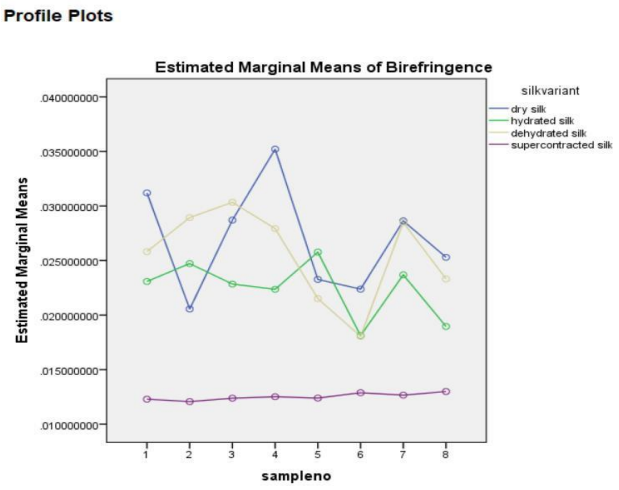

Figure 3.12 Birefringence variation of *Steatoda* silk under four different states

The above plot represents that the dry silk has greater birefringence than any other hydration state but there is a variations in birefringence. When hydration of the silk with both ends were

attached the birefringence decreased considerably. In dehydration state the birefringence increased relatively. In supercontracted state the value of birefringence decreased radically.

Graph 3.13 below represents the fluctuations in the mean value of birefringence of *Steatoda* under different hydration conditions; the error bar represents the variations of data point from the mean value. The standard deviation of each mean is included to represent the variations of silk under different hydration condition.

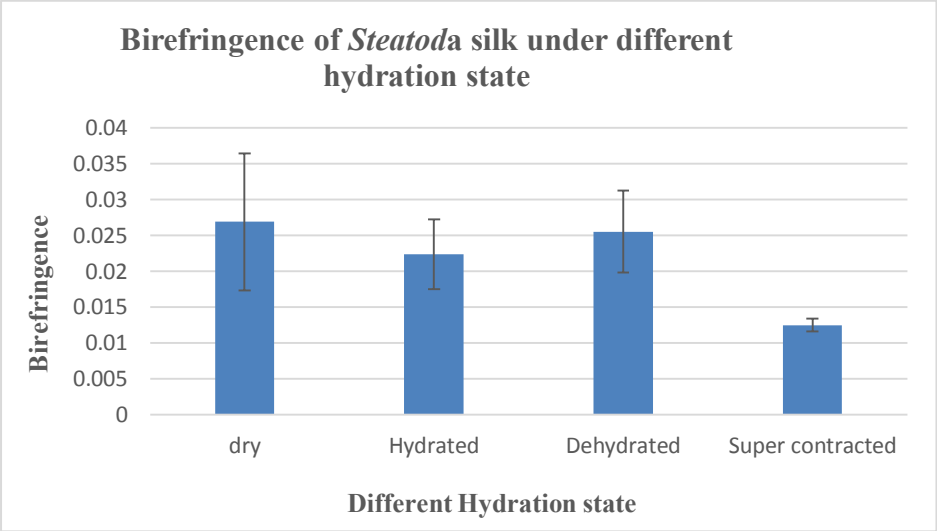

Fure 3.13 Birefringence of *Steatoda* in four different conditions

When comparing the results, the value of birefringence in each condition was significantly different. There was 21% significant decrease in the value of birefringence when the silk was hydrated than in dry state, conversely there was 14% significant increase in birefringence in dehydrated state than in hydration. There was 51% reduction in birefringence when the silk was supercontracted. It is evident that the polarisation state of the silk differs when it gets exposed to various different environmental states. Moreover, we understand that the silk has maximum birefringence when it is in a dry state: on the other hand, the silk has minimum birefringence when it is in a supercontracted state.

3.7 Limitations of the project

Initially, this study was aimed to investigate the correlation between the mechanical properties of the silk and its birefringence. Mechanical testing is usually conducted on engineering

materials, to test whether the material is strong and rigid enough to withstand loads. The tensile strength, is the mechanical property of the material , birefringence is the function of stress and strain in response to changes in the molecular arrangements. Tensile strength, (i.e.) the strength of the material to carry load, whilst being stretched, involves birefringence. The stress and strain curve will be obtained during the tensile test, along with its properties such as: tensile strength, yield strength, elastic modulus, percent elongation, toughness, resilience and Poisson's ratio. These parameters are used to identify and develop new materials and control the quality of materials for efficient use in design and construction. To measure the birefringence of the silk while it elongates under tension, the optical system combined with the tensile stage was expected to be built. However, later it was understood that constructing a tensile device was difficult because, the force required to stretch the fibre was found to be too small, (2 to 5 um thickness) to impose reliably using the available equipment. Furthermore, the diameter of the silk (in the range of 0.001mm to 0.005 mm), required a rather high magnification to resolve properly and thus leaving the tensile measurement extremely vulnerable to sample movement. In addition, the possibility of getting precise measurements using the above assembled optical system, is exceptionally low. For these reasons, it was decided that the custom-assembled system was unsuitable for the purpose of measuring the birefringence of spider silk under the altering conditions of tension. Ultimately, a commercial polarising microscope, BX51 was equipped and a polarisation compensator was accessed within the Materials Engineering group. This met the required measurement needed for this experiment. Initially, it was thought that the commercial Olympus microscope BX51 was capable to determine the tensile strength of the silk, but later it was found that even this commercial microscope was too insensitive to detect strain applied to the silk. Moreover handling the silk in supercontraction state- cutting one edge of the silk, length measurement and positioning the silk on the stage of the microscope was very challenging as the thickness of the silk was in micrometer.

4 Conclusion

Naturally occurring *Nephila* spider dragline silk, has been explored by many researchers for its potential usage in the field of medical, optics and engineering fields. However, this study explored the effect of hydration on a new kind of spider dragline silk known as *Steatoda paykulliana.* Using polarising microscope the birefringence of *Nephila* and *Steatoda* silk in dry state were found. The mean value of thickness of *Nephila* silk is higher than *Steatoda*. Next *Steatoda* silk was undergone different hydration conditions, hydration when restrained, dehydration and supercontraction and the measurement of birefringence were measured in each conditions. The detailed statistical analysis test has been conducted for the experimental results in order to analyse the data. One way analysis of variance was conducted for thickness and Birefringence of *Nephila* silk. The same test has been conducted for *Steatoda* silk's thickness and birefringence measurements. From the test analysis it was found that there were statistically significant difference in thickness and birefringence within individual silk strand and between silk samples, which proves first hypothesis. T test has been conducted for mean value of thickness of *Nephila* and *Steatoda* silk which stated that the thickness of *Nephila* silk is relatively higher than *Steatoda* that confirms second hypothesis. In comparison, the value of birefringence of Hydrated *Steatoda* silk when restrained with previous study by Ken, Savage et al (82), the value of *Nephila* silk was higher than the *Steatoda* silk. Similarly the value of birefringence of supercontraction was higher for *Nephila* than *Steatoda*. One way analysis of variance has been conducted to find is there any variations between the measurements of silk under different hydration conditions - dry, hydration when restrained, dehydration and supercontraction. Birefringence decreases significantly, when the silk was under hydration when restrained. Subsequently, in dehydrated condition the birefringence was increased relatively high, but not reach the value of birefringence of silk in dry state. In supercontraction condition the birefringence decreased drastically nearly half the value of birefringence in dry state. This proves third

hypothesis, in drystate the silk has maximum birefringence. There will be variations in the birefringence of the silk depending upon the level of hydration. The statistical analysis also provides the percentage of variations in different hydration conditions.

From the result, we can conclude that the spider silk can interact with environmental conditions. Different hydration conditions affect the optical property of the silk differently. Birefringence values were higher for dry silk and lower for supercontracted silk. So, this evidences that during hydration there is a modification in the structure of the silk.

These remarkable optical investigations, will allow this promising silk material for future applications , particularly those that involve bio medium. Since the silk has many beneficial properties such as: light propagating properties, optical transparency, remarkable biodegradability, and biocompatibility, we can utilize these material for rendering in industrial, medical and bio photonic applications. In the upcoming years, additional studies need to be conducted subject to optical properties of the silk, to make use of the silk for various purposes. Although spider silk has immense applications, the quantity of the silk retrieved from spiders are very low. It is necessary to find a solution to produce this silk on a larger scale, to manufacture an increased amount of material to use different applications. As the genetic make-up of the *Steatoda* spider silk protein is not known, it is essential for the biological community to study this area. From previous research by (Foong et al., 2020), we get to know that it is possible to produce spider silk proteins using recombinant bacteria (102). This approach to produce silk using recombinant bacteria, will be exceptionally useful to produce huge quantities of spider silk and meet the demand.

Initially this research was aimed to study stress – strain and birefringence characteristics of spider silk. But, not able to set up and find out the optical system with the tensile stage to apply the right force to stretch the fibre. So in future, improvements to the accuracy of the tensile stage system, with further modifications of the experimental setup would be beneficial. Therefore, additional stress – optical characterisation of the spider silk, could possibly be measured.

5 References

1. Kluge J.A. Rabotyagova O, Leisk GG, Kaplan, May 2008. Spider silks and their applications, Trends in Biotechnology, Volume 26, Issue 5, PP.244-251.
2. Borknert B. Christian, Elsnert B. Martina, Scheibel Thomas, 2014. Coatings and Films Made of Silk Proteins, ACS Appl. Mater. Interfaces, 2014, 6(18), pp 15611 – 15625, DOI: 10. 1021/am5008479
3. Teulé F, Addison B, Cooper AR, Ayon J, Henning RW, Benmore CJ, et al, 2012. Combing flagelliform and dragline spider silk motifs to produce tunable synthetic biopolymer fibres. Biopolymers, 97:418-31
4. Lewicka M, Hermanson O, Rising AU, 2012. Recombinant spider silk matrices for neural stem cell cultures Biomaterials, 33:7712-7.
5. Vollrath F, Porter D, 2009. Silks as ancient models for modern polymers. Polymer. 50:5623-32
6. Sponner A, 2007. Spider silk as a resource for future biotechnologies. Entomological Research. 37:238–50.
7. Omenetto, F.G. & Kaplan, D. L, 2008. A new route for silk. Nature Photonics 2, 641 – 643.
8. Omenetto, F.G. & Kaplan, D. L, 2010. New opportunities for an ancient material. Science 329, 528.
9. S. Wright, S. L. Goodacre, 2012. “Evidence for antimicrobial activity associated with common house spider silk”. BMC Res. Notes, DOI: 10.1186/1756-0500-5-326.
10. A.N. Yuri, P.V. Irina, D.I. Lyubov, A.A. Igor, B.G. Vladimir, 2010. “Interaction of recombinant analigs of spider silk proteins 1F9 and 2E12 with phospholipids membranes”. Biochimica et Biophysica Acta (BBA) – Biomembranes, Vol. 1798, Issue 6, pp 1172 – 1178.
11. Gerritsen VB. 2000. An airbus could tiptoe on spider silk. Protein Spotlight. 24:1–2.

12. Vepari. C and David. L.K.K, 2007. Silk as a Biomaterial, Programe Polymer Sci, 32(8-9), 991 -1007.
13. H. Wendt, A. Hillmer, K. Reimers, J. W. Kuhbier, F. Schäfer-Nolte, C. Allmeling, et al., 2011. "Artificial skin–culturing of different skin cell lines for generating an artificialskin substitute on cross-weaved spider silk fibres", *PloS One*, vol. 6, no. 7, pp. e211833.
14. P. Domachuk, H. Perry, J. J. Amsden, D. L. Kaplan, F. G. Omenetto, 2009. "Bioactive self-sensing optical systems", *Appl. Phys. Lett.*, vol. 95, no. 25, pp. 253702.
15. Lawrence B. D, Seryx Processing of *Bombyx mori* silk for biomedical applications Biomedical Inc., USA DOI:10.1533/9780857097064.1.78
16. Wongpanit, P., Pornsunthorntawee, o. & Rujiravanit, R. 2012. CHAPTER 11 Silk Fibre Composities. In John, M. J. & Sabu, T. (eds) Nat. Polym. Vol. 1 Compos. Vol. 1. Chap. Silk Fibre, 219 -256 (The Royal Society of Chemistry).
17. Ingi Agnarsson, Dhinojwal. A, Sahni. V, Blackledge, AT, 2009. Spider as a novel high-performance biomimetic muscle driven by humidity, Journal of Experimental Biology, 212.
18. V. M. Swinerd, A. M. Collins, N. J. Skaer, T. Gheysens, S. Mann, 2007. "Silk inverse opals from template-directed β-sheet transformation of regenerated silk fibroin", *Soft Matter*, vol. 3, no. 11, pp. 1377-1380.
19. Radtke.Christian, Christina A. Heinz Waldmann. K. Reimers, Thies, K et al, 2011. Spider Silk Constructs Enhance Axonal Regeneration and Remyelination in long Nerve Defects in Sheep, PLOS ONE, 6(2), e16990.
20. Chapter Three - Multimodal Communication in Wolf Spiders (Lycosidae), 2016. An Emerging Model for Study G.W.UetzD.L.ClarkJ.A.Roberts Advances in the study of Behaviour United states .Volume 48, Elsevier Inv.pages 117-159.
21. R. Capelli et al., 2011. "Integration of silk protein in organic and light-emitting

transistors", *Organic Electron.*, vol. 12, no. 7, pp. 1146-1151.

22. S. Toffanin et al., 2012. "Low-threshold blue lasing from silk fibroin thin films", *Appl. Phys. Lett.*, vol. 101, no. 9, pp. 091110.
23. R. R. da Silva et al., 2013. "Silk fibroin biopolymer films as efficient hosts for DFB laser operation", *J. Mater. Chem. C*, vol. 1, no. 43, pp. 7181-7190.
24. Huby N et al. 2013. The Native silk as a biological optical fiber. Hal Archives, 102(12), pp.123702.
25. C. Müller, M. Hamedi, R. Karlsson, R. Jansson, R. Marcilla, O. Inganäs, 2011. "Woven electrochemical transistors on silk fibers", *Adv. Mater.*, vol. 23, no. 7, pp. 898-901.
26. J. Gosline, P. Guerette, C. Ortlepp, K. Savage, 1999. "The mechanical design of spider silks: From fibroin sequence to mechanical function", *J. Exp. Biol.*, vol. 202, no. 23, pp. 3295-3303.
27. Lorang D.J., Tanaka D., Spadaccini C.M., Rose K.A., Cherepy N.J., Lewis J.A, 2011. Photocurable Liquid Core–fugitive Shell Printing of Optical Waveguides. Adv. Mater. 23:5055–5058. doi: 10.1002/adma.201102411.
28. Nizamoglu S., Gather M.C., Humar M., Choi M., Kim S., Kim K.S., Hahn S.K., Scarcelli G., Randolph M., Redmond R.W., et al. 2016. Bioabsorbable Polymer Optical Waveguides for Deep-Tissue Photomedicine. Nat. Commun. 7:10374. doi: 10.1038/ncomms10374.
29. Kujala S., Mannila A., Karvonen L., Kieu K., Sun Z. 2016. Natural Silk as a Photonics Component: A Study on its Light Guiding and Nonlinear Optical Properties. Sci. Rep. 22358. doi: 10.1038/srep22358.
30. Tow, K.H., Chow, D.M., et al., 2018. Exploring the use of Native Spider Silk as an Optical Fiber for Chemical Sensing: Journal of Light wave Technology, Vol 36., P (1138 – 1144
31. Chow, D.M., Tow, K.H., Vollrath. F., Dicaire, I., Gheysens, T., and Thevenaz, L., 2015.

Shedding light on the optical properties of spider silk fiber, Proc. IEEE Photonic Conference 2015, 333-334.

32. Parker S.T., Domachuk P., Amsden J., Bressner J., Lewis J.A., Kaplan D.L, 2009. Omenetto F.G. Biocompatible Silk Printed Optical Waveguides. Adv. Mater. 21:2411–2415. doi: 10.1002/adma.200801580.
33. Coddington A.J. Phylogeny and classification of spiders [online]. 2005, Ubick, Spiders of North America: an identification manual. Paguin D. P, Cushing P. E and Roth. V American Arachnological Society. pp: 18 [viewed 22 september2017]. Available from: https://entomology.si.edu/StaffPages/Coddington/2005_Cod.dingtonSNAPhylogeny.pdf.
34. Lazaris A, et al., January 2002, Spider silk fibers spun from soluble recombinant silk produced in mammalian cells, Science, 18; 295(5554):472-6
35. J.M. Gosline, M.E. Demont, and M.W. Denny. 1986, "The Structure and Properties of Spider Silk". In: Endeavour 10, pp.37–43.
36. Anderson .M, Holm. L, Ridderstrate. Y, Johansson. J and Rising. A. 2013. Morphology and Composition of the spider Major Ampullate Gland and Dragline Silk, Biomacromolecules 14(8) pp 2945-2952.
37. Coddington, J A. 1989. Spinnerets silk spigot morphology: Evidence for the monophyly of orb-weaving spiders, Cyrtophorinae (Araneidae), and the group Theridilidae plus Nesticide. J. Arach-nol., 17:71-95.
38. Romer. Lin and Thomas Scheibel, 2008. The elaborate structure of spider silk structure and function of a natural high performance fiber, Prion 2(4), 154-161C.
39. S. Vasav, B. Todd A, D. Ali, 2011, Changes in the Adhesive properties of Spider Aggregate Glue during Scientific Reports. DOI: 10.1038/srep00041.
40. Babb. L. P, Lahens. F. N, et.al, 2017, The *Nephila clavipes* genome highlights the diversity

of spider silk genes and their complex expression, Nature Genetics, 49, 895-903.

41. Boutry and T.A. Blackledge. 2008. “The Common HouseSpider Alters the Material and Mechanical Properties of Cobweb Silk in Response to Different Prey”. In: Journal of Experimental Zoology Part a-Ecological Genetics and Physiology 309A, pp. 542–552.
42. K. H. Guehrs, B. Schlott, F. Grosse, and K, 2008, Weisshart. “Environnemental conditions impinge on dragline silk protein composition”. In: Insect Molecular Biology17, pp.553–564 T. Scheibel. 2004, “Spider silks: recombinant synthesis, assembly, spinning, and engineering of synthetic proteins”. In: Microbial Cell Factories3, p.14.
43. Nentwig W. Why do only certain insects escape from a spider's web? Oecologica. 1982; 53:412–417R.W. Work. 1976, “Force-Elongation Behaviour of Web Fibers and Silks Forcibly Obtained from Orb-Web-Spinning Spiders”. In: Textile Research Journal46, pp.485–492.
44. Dai L., Zhang Y., Ou Yang Z., 2003, Thin film solids, 438-439, 382-285.
45. Vollrath F, Tillinghast EK. 2005, Glycoprotein glue beneath a spider web's aqueous coat. Naturwissenschaften, 78:557–559 M. Denny. 1976, “Physical properties of spider silk and their role in design of orb-webs”. In: Journal of Experimental Biology 65, pp.483–506.
46. Madson B., Vollrath F., 2000, naturwissenschaften, 87,147-153.
47. F. Vollrath and D.P. Knight. 2001, “Liquid crystalline spinning of spider silk”. In: Nature410, pp.541–548.
48. O. Emile, A.L. Floch, and F. Vollrath. 2007, “Time Resolved Torsional Relaxation of Spider Draglines by an Optical Technique”. In: Physical ReviewLetters98, pp.167402/1–167402/4.
49. F. K. Ko and J. Jovicic. 2004, “Modeling of mechanical properties and structural design of spider web”. In: Biomacromolecules 5, pp.780–785.

50. T. Scheibel. 2004, “Spider silks: recombinant synthesis, assembly, spinning, and engineering of synthetic proteins”. In: Microbial Cell Factories3, p.14.
51. R.W. Work. 1976, “Force-Elongation Behaviour of Web Fibers and Silks Forcibly Obtained from Orb-Web-Spinning Spders”. In: Textile Research Journal46, pp.485–492.
52. D. Saravanan, 2006. Spider silk- Structure – Properties and Spinning: Journal of textile and Apparel, technology and Management vol: 5, Issue. Kubik S. High-performance fibers from spider silk. Angew Chem Int Ed Engl. 2002; 41:2721–2723.
53. M. Denny. 1976, “Physical properties of spider silk and their role in design of orb-webs”. In: Journal of Experimental Biology 65, pp.483–506.
54. Perez R.J., Viney C., Llorca J., Elices M., J. 1998, Appl. Poly. Sci., 70, 2439-47.
55. Kubik S. High-performance fibers from spider silk. Angew Chem Int Ed Engl. 2002; 41:2721–2723.
56. Kunal Singha, Subhankar Maity, Mrinal Singha, 2012, Spinning and Application of Spider Silk. Frontiers in Science, -ISSN: 2166-6083, 2(5): 92-100.
57. Vollrath. F, Madsen. B and Shao. Z, 2001.The effect of spinning conditions on the mechanics of a spider’s dragline silk, Proc Biol Sci 22; 268(1483):2339-2346.
58. Vollrath F, knight DP, 2001. Liquid crystalline spinning of spider silk, Nature 410(6828): 541-8.
59. Harun Yahya, may 2001, The Miracle in the spider, New Delhi, The Islamic Centre, pp: 68.
60. .Lucas, F. (1964) Discovery 2, 20 -26Romer. Lin and Thomas Scheibel, 2008. The elaborate structure of spider silk structure and function of a natural high performance fiber, Prion 2(4), 154-161.
61. Witt, P.N., C.E. Reed and D.B. Peakall. 1968. A Spider’s web. Springer Verlag, New York Chapter Vpage 74-89.

62. Hakimi, O.; Knight, D. P.; Vollrath, F.; Vadgama, P, 2007, Spider and Mulberry Silkworm Silks as Compatible Biomaterials. Composites Part B: Engineering., 38, 324–337

63. Catherine L. Craig., Gary D. Bernard., 1990, Insect attraction to ultraviolet reflecting spider web and web decorations Ecology 71(2) pp 616-613.

64. Liu Y, Shao Z, Vollrath F (2005) Relationships between supercontraction and mechanical properties of spider silk. Nat Mater 4: 901–905.

65. Warwicker, J. 1960. Comparative studies of fibroins. II. The crystal structures of various fibroins. J. Mol. Biol. 2:350–362.

66. Li SF, McGhie AJ, Tang SL (1994) New internal structure of spider dragline silk revealed by atomic force microscopy. Biophys J 66: 1209–1212.

67. Knight DP, Knight MM, Vollrath F (2000) Beta transition and stress-induced phase fibre spinning. Nat Mater 4: 772–775.

68. Thiel BL, Guess KB, Viney C (1997) Non-periodic lattice crystals in the hierarchical microstructure of spider (major ampullate) silk. Biopolymers 41: 703–719.

69. Sponner A, Unger E, Grosse F, Weisshart K (2005) Differential polymerization of the two main protein components of dragline silk during fibre spinning. Nat Mater 4: 772–775.

70. Augsten K, Muehlig P, Hermann C (2000) Glycoproteins and skin-core structure in *Nephila* clavipes spider silk observed by light and electron microscopy. Scanning 22: 12–15

71. Shao ZZ, Hu XW, Frische S, Vollrath F (1999) Heterogeneous morphology of Nephila edulis spider silk and its significance for mechanical properties. Polymer 40: 4709–4711

72. Ayoub NA, Garb JE, T RM, Collin MA, Hayashi CY (2007) Blueprint for a High-Performance Biomaterial: Full-Length Spider Dragline Silk Genes. PLoS ONE 2(6): e514.

73. Van Beek JD, Hess S, Vollrath F, Meier BH (2002) The molecular structure of spider dragline silk: folding and orientation of the protein backbone. Proc Natl Acad Sci U S A 99: 10266–10271.

74. Madurga R et al, 2016, Material properties of evolutionary diverse spider silks described by variation in a single structural parameter, Scientific Reports 6:18991.

75. Marsh, R., R. Corey, and L. Pauling. 1955. An investigation of the structure of silk fibroin. Biochim. Biophys. Acta. 16:1–34.

76. Glisovic, A., and T. Salditt. 2007. Temperature dependent structure of spider silk by X-ray diffraction. Appl. Phys. A. 87:63–69.

77. https://www.microscopyu.com/techniques/polarized-light/principles-of-birefringence

78. Felice De Santis and Roberto Pantani (2013) Optical Properties of Polypropylene upon Recycling, The Scientic World Journal, Volume 2013, Article ID 354093, 7 pages.

79. Douglas J.Little , Kane.D.M, (2011) Image contrast immersion method for measuring refractive index applied to spider silk, Optics Express, Vol 19, Issue 20, pp; 19182-19184.

80. Douglas little and Deborah Kane, October 15, (2011) Hybrid immersion-polarization method for measuring birefringence, Optics Letters, Vol 36, No. 20.

81. Chris Holland, Kathy o' Neil, Fritz Vollrath, Cedric Dicko, 2012. Distinct structural and optical regimes in natural silk spinning – Journal Biopolymers, Vol 97, Issue 6, pp:368-373.

82. Ken N. Savage and John M. Gosline. 2008, "The effect of proline on the network structure of major ampullate silks as inferred from their mechanical and optical properties". The Journal of Experimental Biology 211, 1937 -1947 doi: 10.1242/ jeb.014217.

83. QIOPTIQ. The LINOS Light Sources and Lasers [online]. [Viewed 20 September 2017]. Availablefrom:http://www.qioptiq-shop.com/out/pictures/wysiwigpro/12-13%20englisch/21%20Light%20Sources%20and%20Laser.pdf

84. Thorlabs, Inc. [US], [online]. [Viewed 20 September]. Available from: http://www.Thorlabs.com/new group page 9.cfm? object group_id=4024.

85. Thorlabs, Inc. [US], [online]. [Viewed 20 September 2017]. Available from: https://www.thorlabs.com/thorProduct.cfm?partNumber=DCC1645C.

86. http://olympus.magnet.fsu.edu/primer/techniques/polarized/configuration.html

87. http://olympus.magnet.fsu.edu/primer/java/compensators/berek/index.html

88. Kadam. P, Bhalerao S., 2010. Sample size calculation, Int J Ayurveda Research 1(1): 55-57

89. Work, R.W. 1981. A comparative study of the Supercontraction of major ampullate silk fibers of orb-web-building spiders (Araneae). J. Arachnol., 9:299-308.

90. Jiang P, Guo C, Lv T, Xiao, Liao X and Zhou B, "Structure, composition and mechanical properties of the silk fibers of the egg case of the *Joro* spider, *Nephila clavata* (Araneae *Nephilidae,*). J. Biosci 36 897 -910 DOI 10,1007/s12038-011-9165-3

91. Gatesy J, Hayashi C, Motriuk D, Woods J, Lewis R, 2001, Extreme diversity, conservation, andconvergence of spider silk fibroin sequences. Science, 291: 2603-2605. 0.1126/science.1057561

92. Rickel. C, Muller. M, Vollrath. F, 1999, Macromolecule, 32(13) (1999)

93. Tillinghast. E. S, Chase.S. F, Townley. M. A. 1984, Insect Physiol., 30(7) (1984), pp 591-596.

94. Olena Tokareva,[1,&] Matthew Jacobsen,[2] Markus Buehler,[3] Joyce Wong,[2] and David L. Kaplan

2014.Structure-Function-Property-Design Interplay in Biopolymers: Spider Silk, Acta Biomater. 10(4): 1612-1626.

95. Liu Y[1], Shao Z, Vollrath F. 2005, Relationships between supercontraction and mechanical properties of spider silk, Nat Mater, 4(12): 901-5.

96. Rickel. C, Muller. M, Vollrath. F, 1999, Macromolecule, 32(13).

97. Gosline, J.M, M. W. & Demont, M.E, Spider silk as rubber. Nature 309,551-552.

98. Boutry. C and Blackledge. TA, 2010, Evolution of supercontraction in spider silk: structure-function relationship from tarantulas to orb-weavers. J Exp Biol, 213(pt 20): 3505-14.

99. Tokareva.O, Jaconsen M., Buehler M., Wong J., Kaplan L.D, 2014, Structure –Function–Property-Design Interplay in Biopolymers: Spider Silk. Acta Biomator 10(4): 1612-1626.

100. Choon Pin Foong et al. A marine photosynthetic microbial cell factory as a platform for spider silk production, Communications Biology (2020).

101. C.B.Lin, Yi-Ting Lee and YangLiu, 2020, Spider silk can create lenses useful for Biological Imaging, Journal of Applied Physics, DOI: 10.1063/5.0007611

Appendix

Experimental value of birefringence of *Steatoda* spider silk in four different conditions –dry, hydration with restrained, dehydration, Supercontraction were tabulated below

Birefringence of *Steatoda* under four different conditions

Sample	Location	Dry	Hydration	Dehydration	Supercontraction
1	A	0.022387435	0.024984925	0.028127536	0.011866055
1	B	0.023686047	0.01831954	0.024969121	0.012054902
1	C	0.047526846	0.025943925	0.024362319	0.012963636
2	A	0.019382199	0.014504823	0.028463158	0.012870036
2	B	0.022387435	0.030631579	0.02467128	0.010024444
2	C	0.019908046	0.029034483	0.033692308	0.013321569
3	A	0.027956376	0.022205128	0.028697987	0.012054902
3	B	0.043840467	0.018376947	0.037842697	0.012365201
3	C	0.014329843	0.02795637	0.024482315	0.012722846
4	A	0.021165109	0.020722846	0.03188764	0.012535055
4	B	0.041926174	0.022819095	0.025078652	0.012963636
4	C	0.042539683	0.023544987	0.026817416	0.012054902
5	A	0.015194079	0.022681159	0.025943925	0.01086988
5	B	0.016895131	0.032669065	0.016895131	0.013449309
5	C	0.037724868	0.021980337	0.021701342	0.012861925
6	A	0.024707547	0.016895131	0.016895131	0.011314928
6	B	0.020722846	0.021613281	0.020381323	0.012835073
6	C	0.021701342	0.01582807	0.016895131	0.0145
7	A	0.024464419	0.022387435	0.034525333	0.012345382
7	B	0.027437209	0.021701342	0.022307463	0.013065385
7	C	0.034014981	0.026991304	0.028661539	0.012572597
8	A	0.026195767	0.014458333	0.029438849	0.013203704
8	B	0.024739837	0.020722846	0.019145329	0.012572597
8	C	0.024955056	0.021701342	0.021379592	0.013203704
Mean		0.026907864	0.022444762	0.025552605	0.012524653
SD		0.00953478	0.004872819	0.005728214	0.00091748

Internal Examiner

1. In page 26 of the thesis, the Author quoted the Malus's Law saying that the light intensity after the analyser is given by I = I0 cos2θ. A paragraph later, the Author gave a second expression for the light intensity after the analyser, which was Ia ~ sin2 (2θ). Mathematically the expressions are not the same, and one does not lead to the other, and the two described very different situations: according to the first one, the light intensity goes through a bright/dark cycle every 1800 , whereas for the second one, it is every 900 . Also, the first one indicates that the light intensity is bright at θ = 00 , but the second one suggests that at θ= 00 , the output is dark

   Answer : Malus law has been explained in Chapter 1, section 1:8 Principle of Polarised

   Light Microscope - page 13 & 14

   The output intensity when the silk was present under crossed polarisers, was explained

   in Chapter 1, section 2.4 Spider silk under polarised light – Page 27 & 28

2. I could not find any mention of the orientation of the optical axes of the fibre relative to the axes of the polariser, which would influence the measurements. Imagine if the pass axis of the polariser is parallel to one of the axes of the fibre, rotating of the analyser will have no effect on the intensity of the light.
   Answer: 2:4 Spider silk under polarised light section. (Page 29)

3. Near the bottom of page 2, it was said that "Most importantly birefringence of the silk because this is one of the most important optical property". Why was the birefringence one of the most important optical property, in relation to the applications considered in the thesis?
   Answer: Section 1:1 Introduction Page 2

4. The qualities of the images of the hair are generally very poor (say figure 2.2 & 2.4). It was suggested that their contrast was degraded due to unwanted ambient lighting. If that was the case, why wasn't the experiment repeated with the ambient lighting excluded from the camera? This could be done by drawing the curtains, switching off of the room light, putting on the enclosure covering the set up. All very simple exercises which would give readers the confidence on your experiment.
   Answer: This has been rectified in the next part of the experiment, when I placed the polariser and analyser. I enclose the optical system by a black sheet in order to avoid ambient light.
   Section 2:3.3 Construction of optical system stage II, page no 26 & 27.

5. The explanation for figures 2.6 & 2.7 are very confusing. Did you alter the orientation of the analyser between the two figures in order to effect the change in contrast? Looking at the brightness of a picture may not give a reliable indication to the actual contrast.

Showing a line profile across the relevant features would.

Answer: Line profiles were drawn . Section 2.4 Spider silk under polarised light, page 30. Ref : Fig 2.9 & Fig 2.10.

6. Why did figures 2.6 & 2.7 has a larger magnification than that in figures 3.1 & 3.4? one would have thought for measurement purpose, large magnification should be preferred. Why was the silk used in figure 2.6 appeared so much wider than that in figure 3.1? After all both are Nephila silk.

   Answer: In figure 2.6 and 2.7 , the images were taken from my assembled microscope and I have set up 200x magnification for that constructed optical system. The figure 3.1 & 3.2 were taken from Olympus microscope with magnification of 100x . When I tried to increase the magnification of the silk image but the contrast of the image was decreased and the image appeared blurry. Section 2.6. Measurement of birefringence of Nephila clavipes spider silk. Page 35.

7. The measured parameters in chapter 3, and in the tables as well, they all have error bars associated with them. How was the error obtained? Did you repeat the same measurement many times to get the error bars?

   The error bars represents the variations of data points from the mean value. Page 44, page 45 and page 54.

8. The Berek compensator (figure 2.0, page 30) would really benefit from a diagram showing the orientation of the optical axes relative to the rest of the system. It would make the explanation so much clearer and easier to understand.

   Answer: The figure has added now.

   Section 2.5.2 Berek Compensator, Fig: 2:10, Page 33.

9. The Author offered no design considerations in the thesis at all. For example, why was a magnification of x200 chosen? What was the lateral resolution required for the spider silk? What determined the precision of the measured parameters? Was the measurement repeatability good enough for the application? It appeared that the Author set up a system with some available components, without any consideration whether the system was suitable for the application

   The design consideration was written in section 2.3 Construction of polarised light microscope

   – page 20 & 21
   Lateral resolution 2.3.1 – Required components and their specifications – page 23

10. What determined the precision of the measurements.
    Section 3.1 Birefringence and thickness of *Nephila* Spider dry dragline silk – Standard deviation , significant figures- Page 43
    Section 2.7 Sample Size -page 38

External Examiner

1. "between and within the silk sample" makes no sense.
   This has been corrected as within individual silk samples and between discrete / distinct silk samples.
   Corrected all over the place Chapter I, chapter 11 and Chapter111

2. My version had bookmark errors in the contents. "Error! no bookmark found"
   Corrected.

3. not being cause to any allergic reactions to humans". Confusing.
   corrected .Section 1.1 introduction- Page 1

4. Order names should not be italicised.
   Corrected. Section 1.2 Spider silk , Page 3

5. Incorrect presentation of species names: Genus first letter capitalised, species not.
   Corrected:. All over the place

6. Spider silk has been recognised for more than two millennia, not two decades.
   Corrected – 1.2 Spider silk, page 3

7. There is a lot about orb-weavers but *Steatoda* is not an orb-weaver. How far is the introductory material relevant to the actual study species?
   Section 1.2 Spider silk , Page 3, 4, *Steatoda* spin tangled web
   Section 3.2 Thickness and birefringence variations of Steatoda silk– Comparing thickness and birefringence measurement of *Nephila* and *Steatod*a, Page 46, 47
   Section 3.3 Birefringence of *Steatoda* hydrated when restrained – comparing optical properties of *Nephila* and *Steatoda*
   Section 3.5 Steatoda silk under supercontraction , comparing birefringence measurement of *Steatoda* with *Nephila* page no 50 & 51

8. Amino acids are the monomers, they are not made up of monomers.
   Corrected -Section 1.5 Spider silk composition -page no 9

9. Aims: how is *Steatoda* a novel spider?
   Introduction 1.1, Page 1

10. Methods. Hydrated with restrain? Not clear at all. This needs to be made much clearer. Is the word "restrain" or "restrained" here?
    Corrected as restrained – all over the place

11. "When restrained" rather than "with restrained"
    Corrected

12. The figures are extremely simple and not well rendered.
    Made changes in Section 1.1, 1.3and 1.4 Page 4, 5, 6 and 8